1969, *Bull. Astr. Inst. Netherlands* **20** 225-273; *Communication from the Observatory at Utrecht*

ON THE SPECTRUM AND NATURE OF P CYGNI

MART DE GROOT

Received 16 December 1968

From a study of 36 high-dispersion spectrograms of P Cygni covering the period from 1942 to 1964 it is found that many of the absorption lines are double and the hydrogen absorption lines are triple. All absorption components are displaced to shorter wavelength. This is attributed to line formation in different shells in an expanding atmosphere. Wavelengths and identifications for all observable lines are given together with the radial velocities and equivalent widths for the hydrogen, the helium and some other important spectral lines. In the outer shell the radial velocity varies from −180 to −240 km/sec with a period of 114 days. It is concluded that the velocity of expansion of the atmosphere of P Cygni increases from 50 km/sec at the stellar surface to more than 200 km/sec at a distance of 3 stellar radii from the surface. Several atmospheric parameters are derived: the electron density varies around an average value $\log N_e = 12.76$; the geometrical thickness of the outer shell is four times that of the two inner shells together and its distance from the star's centre is about 3.5 stellar radii. The mass loss is rather high: $2.0 \times 10^{-4}\ M_\odot$/year. The spectroscopic data do not confirm the conclusion of Magalashvili and Kharadze that P Cygni is a W UMa star, nor that of Fernie that it is a β Cephei star. Pulsational instability is suggested as the reason for the observed light variations. The propagation of sound waves generated by the pulsational instability may be important in understanding how the observed phenomena should be explained.

1. Introduction

The star P Cygni (HD 193237, α (1900) = $20^h14^m.1$, δ (1900) = $+37°43'$, $m_v = 4.88$) has given its name to a class of stars with peculiar spectra. The spectra of these so-called "P Cygni-type stars" are characterized by the presence of spectral lines consisting of a nearly undisplaced emission component accompanied by one or more shortward displaced absorption components. This phenomenon has always been explained by the assumption of an expanding atmosphere around the star.

The characteristic "P Cygni" features are most completely shown by P Cygni itself: the vast majority of the spectral lines show the "P Cygni" character. Because of its apparent brightness P Cygni lends itself for a careful study of its spectrum which in principle contains all the information about the state of motion and the excitation and ionization conditions in the expanding atmosphere. It is hoped that the results of such a study will give us information about the P Cygni stars in general, although P Cygni itself is not really a type star. Most of the P Cygni stars are classified as late B- or early A-type stars, whereas the spectral type of P Cygni according to the absorption lines is given as B1p in the Henry Draper Catalogue, as B1qk in the Revised Victoria System and as P Cyg in the MK system.

With respect to the simultaneous presence of absorption and emission lines P Cygni-type spectra resemble those of novae in a certain stage of evolution. In fact, P Cygni itself is an old nova that was discovered on Friday, August 18th of the year 1600 by the Dutch chartmaker, geographer and mathematician Willem Janszoon Blaeu. Although the records about celestial phenomena were neither accurate nor complete in those days, it seems clear that the star reached its maximum brightness of the third magnitude quite suddenly. Nevertheless there is no complete agreement upon the nova character of P Cygni because the star remained at maximum brightness for about six years. After 1606 the luminosity slowly decreased until P Cygni became invisible to the naked eye in 1626. From 1654 to 1656 it brightened again and remained of the third magnitude until 1659. Between 1660 and 1683 P Cygni was of varying brightness, sometimes it could be seen as a faint star, sometimes it became invisible to the naked eye and even in a small telescope. After 1683 the

brightness slowly increased until magnitude 5.4 was reached in 1715 and magnitude 5.2 in 1780. From 1780 to 1870 the brightness remained constant, except for the period from 1781 to 1786 when the star seems to have been about 0.4 magnitudes fainter. After 1870 there was another slow increase in brightness to magnitude 4.9. In more recent years the application to the determination of stellar magnitudes of modern photoelectric techniques has yielded much more accurate information on the brightness of P Cygni. From these modern observations it is now clear that P Cygni shows irregular brightness variations with a maximum amplitude of about 0.2 magnitudes. A fairly complete bibliography about all investigations concerning P Cygni up to 1954 has been given by SCHNELLER (1957). Quite recently MAGALASHVILI and KHARADZE (1967a, b) have presented some evidence that the light variations of P Cygni are not completely irregular: the star might be a W UMa-type variable. This subject will be discussed more fully in section 6.

Measurements of the colour of P Cygni have been made as early as 1602, but in view of the fact that various observers used different descriptions for the colour it is not possible to deduce from those early observations how the colour of P Cygni has changed. Only one thing is certain in this respect: all observers agree that P Cygni is a reddish star, which is remarkable in view of its early spectral type.

As early as 1897 it was found that the spectrum of P Cygni presented the above mentioned double character of the spectral lines, which at first was interpreted as an overlapping of two different spectra. Between 1888 and 1911 several observers studied the spectrum of P Cygni. MERRILL (1913a) did not include P Cygni in a list of stars with variable spectra nor in a list of stars with spectra suspected of variability. This represents the conclusion of several observers none of whom ever had found variations in the spectrum of P Cygni. However we should keep in mind that the spectrograms of those days did not have a quality comparable to what could be obtained in later years. Therefore, the early conclusion of the non-variability of the spectrum of P Cygni is not really a proof that nothing has changed; but the variations must have been small.

In 1913 MERRILL (1913b) was the first investigator who reported something about spectral variations in P Cygni after a study of spectrograms obtained with the Lick three-prism spectrograph in 1912 and 1913. FROST (1912) on the contrary concluded from a series of spectrograms obtained between 1904 and 1912 that there were no variations in the spectrum of P Cygni. This illustrates the remark made in the previous paragraph about the difficulty of detecting small spectral variations. Even LOCKYER (1924) and ELVEY (1928) state that the spectrum of P Cygni shows no variations on their spectrograms. But Lockyer finds that all absorption lines are single while Elvey finds that some absorption lines are double which, however, he attributes to instrumental errors.

The problem of how to interpret the spectrum of P Cygni came a bit closer to a solution with the work of BEALS (1930a, b; 1932; 1934; 1935). He explained the P Cygni-type spectral lines in novae, Wolf-Rayet stars and P Cygni as due to a radially expanding atmosphere around the star. STRUVE (1935) in a detailed discussion added much physical interpretation of the excitation and ionization in the atmosphere of P Cygni to the more geometrical discussion of Beals. One of the latest extensive studies of P Cygni is the paper in which BEALS (1950) discusses some 69 stars with P Cygni-type line profiles in their spectrum. Further references to earlier work on the spectrum of P Cygni are given by SCHNELLER (1957) and by UNDERHILL (1966). Among the most recent investigations are those of LUUD (1966, 1967a, b) about the variations of the continuous spectrum and about the spectral variations in 1964, 1965 and 1966.

The purpose of this investigation is to give a detailed account of the many spectral peculiarities shown by

TABLE 1

Characteristics of the spectrographs

Observatory	Telescope and spectrograph	Dispersion (A/mm)	Number of spectrograms
Haute Provence	76-inch coudé		
	chambre IV	9.7	2
Lick	120-inch coudé	2.0	6
Mt. Wilson	100-inch coudé	2.9	14
		4.5	2
		9.0	1
		10.3	3
		20.5	3
Dominion	48-inch coudé		
Astrophysical	32122	4.9	3
(Victoria)	32121	10.2	1
	3262	8.7	1

P Cygni, including line intensities and radial velocities. In the second and third sections the observational material and the way it was reduced are described. The results from the study of the spectrograms are given. These results, radial velocities and line profiles, are discussed in sections 4 and 5. Section 6 is a discussion of the light variations of P Cygni. It is attempted to construct a model for the atmosphere of P Cygni. A number of conclusions and some suggestions for future work form the contents of the last section.

2. The observational material

The observational material consists of high-dispersion spectrograms obtained with different instruments at various observatories. The main characteristics of the spectrographs used are listed in table 1. The columns give the name of the observatory and of the spectrograph, the dispersion and the number of spectrograms from each instrument used in this investigation. All of the listed instruments are grating spectrographs. The spectrograms cover the period from July 1942 to November 1964. Not all spectrograms were used for all parts of this investigation. A few overexposed and some brownish spectrograms (probably due to incomplete fixing during the photographic process) were used for radial-velocity determinations only and not for de-

TABLE 2

Spectrograms of P Cygni used in this study

Plate number	J.D.–2430000 (U.T.)	Date (U.T.)	Wavelength region studied	Purpose for which used
Mt. W. 2820[1,2]	543.928	1942 July 2	3530–4030, 4070–4730	radial velocities, line profiles
2832[1,2]	570.785	July 29	3630–4200, 4325–4875	radial velocities, line profiles
2877[1,2]	630.815	Sept. 27	3650–4260, 4300–4875	radial velocities, line profiles
2894[1,2]	662.712	Oct. 29	3650–4230, 4325–4875	radial velocities, line profiles
3040a	865.930	1943 May 23	3100–4500	radial velocities
3040b	865.994	May 23	3600–5200	radial velocities
3113	925.877	July 19	3500–5200	radial velocities
3114	925.959	July 19	5850–8800	radial velocities
3227	1009.665	Oct. 11	5850–8800	radial velocities
3446[1,2]	1254.967	1944 June 12	3650–4350, 4375–4950	radial velocities, line profiles
3776[1,2]	1578.955	1945 May 2	3650–4300, 4330–4950	radial velocities, line profiles
3963[1,2]	1715.751	Sept. 16	3700–4350, 4375–4875	radial velocities
3999	1727.625	Sept. 28	4400–6700	radial velocities
5388	2845.753	1948 Oct. 20	5100–6500	radial velocities
8118a	4178.997	1952 June 14	3650–5020	radial velocities
8118b	4179.003	June 14	3450–5020	radial velocities
8818	4591.963	1953 Aug. 1	3700–4475	radial velocities
8824	4593.945	Aug. 3	3700–4475	radial velocities
Lick EC-221[a,b]	7154.760	1960 Aug. 8	3150–3475, 3540–4025	radial velocities, line profiles
EC-228[a,b]	7155.747	Aug. 9	3150–3475, 3530–4030	radial velocities, line profiles
EC-230[a,b]	7155.886	Aug. 9	3530–4040, 4050–4500	radial velocities, line profiles
O.H.P. W 1938	8249.629	1963 Aug. 7	3500–5050	radial velocities
W 1940	8251.583	Aug. 9	3450–5050	radial velocities
D.A.O. 1520	8659.651	1964 Sept. 21	3275–4050	radial velocities
1544	8673.629	Oct. 5	3475–4050	radial velocities
1545	8673.715	Oct. 5	3175–4075	radial velocities
1551	8674.678	Oct. 6	5600–6700	radial velocities
1610	8724.571	Nov. 25	3500–5100	radial velocities

ducing line profiles. Most of the spectrograms are well exposed and are free from guiding streaks. Only the spectrograms with the highest dispersion were used for obtaining line profiles. Table 2 lists the plate numbers, date of observation, wavelength region studied and the purpose for which each spectrogram was used.

Most of the Mount Wilson spectrograms have already been the subject of a study by W. S. Adams. But at the time of his death in 1956 he had only been able to measure and to tabulate radial velocities for the absorption and emission components of the stronger lines. The material was then prepared for publication by Merrill (ADAMS and MERRILL, 1957) who also gave some microphotometer tracings of various spectral lines; but Merrill hardly discussed the results. A closer and more extensive study of these spectrograms has revealed many interesting features that may contribute to a better understanding of the atmospheric structure of P Cygni.

3. The measurements

Two different kinds of measurement were made. The first was for obtaining accurate wavelengths for each spectral feature and radial velocities of the major lines in the spectrum. The second was for obtaining intensity profiles of all the major spectral lines. The way in which these two different kinds of measurement were carried out is described in the next two sections.

3.1. *The wavelength and radial-velocity measurements*

On all of the plates accurate wavelength measurements were made with the Zeiss Abbe Comparator of the Utrecht Observatory. For greater ease and comfort of measuring, magnified images of the spectrum and of the scale were projected on a white paper. Looking at the spectrum in projection is less tiring for the eye than viewing it through a microscope. Therefore it is possible to detect very faint spectral features even after some time of measuring. This is the main reason why projection is to be preferred to viewing the spectrogram directly with a microscope.

The measured wavelengths were used for drawing a wavelength scale on the microphotometer tracings. The sharp interstellar lines and the symmetrical stellar spectral lines were used as zero-points of wavelength on the tracings. Only for these lines can one be certain about the coincidence of a wavelength measurement with the comparator and one made on the tracing. From a comparison of table 4 with the registration for a single spectrogram it is found that all the lines that are found when measuring that spectrogram on the measuring machine are those lines in table 4 with intensities greater than 0. Of the lines in table 4 with intensities equal to 0, about 2/3 are found on the tracing when it is inspected. About 1/3 are not found, but there is an equal amount of very weak lines found on the tracing that are not in table 4. The general conclusion from this comparison is that all the lines in table 4 with intensity greater than 0 are real spectral lines, whereas of the lines with intensity equal to 0 two thirds are real and one third probably is not.

Since the radial velocity derived from various spectral lines varies with time (cf. section 4) it is not possible to compile a list of measured wavelengths together with their identification. On the other hand, such a list would prove helpful for future work on the spectrum of P Cygni and similar stars. Therefore it was decided to average all wavelength measurements of all individual lines and to give these wavelengths together with their possible identifications.

3.1.1. The identifications

Table 3 summarizes the spectra that were identified in the spectrum of P Cygni. No search was made for spectra not listed in this table. The wavelengths and identifications are presented in table 4 in which the first four columns contain information about the observed lines. Column 1 gives the mean of the wavelength measurements on several spectrograms. Column 2 gives the

TABLE 3

Spectra identified in the spectrum of P Cygni

Present	Probably present	Possibly present	Probably not present
H, He I, C II, N II, N III, O I, O II, Na I, Mg II, Si II, Si III, Si IV, S III, Ar II, Ca II, Fe III, Ni II	C III, Ne II, Ca III	Ne I, Na II, Al III, Cl III	He II, Li I, Li II, Be II, B II, B III, C IV, O III, F II, F III, Al II, P II, P III, S II, Cl II, Ar III, K I, K II, K III, Ca I, Ti II, V II, Cr II, Mn II, Fe II
Interstellar lines			
Na I, Ca I, Ca II, Ti II, CH^+	Fe I, CH	K I	Ti I, V I, Cr I, Mn I, Fe II, Ni I, CN

nature of the observed feature; a means absorption, e means emission; sometimes there is a second letter, s meaning a line that is much sharper than most of the other lines and n meaning a line that is much wider than most of the other lines. Column 3 gives the mean intensity of the line. This intensity was estimated while measuring the spectrograms with the Abbe Comparator using a scale of intensities in which 0 means a line at the limit of visibility, 0.5 is for lines which are in all probability present, and 1.0 and up for lines the presence of which is beyond doubt. Column 4 gives the number of plates from which the mean wavelength and intensity were determined. If two or more lines are believed to form part of one greater feature, those lines are connected by round brackets just behind the number in column 4. This is the case for all lines that show P Cygni-type profiles with an absorption and an emission component. Columns 5, 6 and 7 contain information about the identifications. Unless otherwise stated the wavelengths and multiplet numbers are from the *Revised Multiplet Table* (MOORE, 1945; in what follows to be abbreviated as R.M.T.). However, since the publication of the R.M.T. the results of more accurate and more extensive investigations of a number of spectra of ions have become available. These later results have been used as much as possible. Column 5 gives the laboratory wavelength, column 6 gives the spectrum and column 7 gives the multiplet number for those spectra that were taken from the R.M.T. Column 8 is for remarks and some other information. For many observed lines more than one identification is possible. For these lines all different possibilities are listed in order of increasing wavelength and the line which is believed to be the most important contributor to the blend has an asterisk (*) in column 8. In a few cases where it is very doubtful which line is the most important the asterisk has been omitted. In some other cases where more than two identifications are possible it proved difficult to decide between the two strongest contributors. In these cases these two strongest lines both have an asterisk. The interstellar lines are indicated by the symbol IS in column 8. For some identifications it was thought necessary to give an explanation or a remark. A letter R refers to those remarks which are listed in order of wavelength at the end of table 4.

H: The lines from Hα to H30 are visible on the best exposed spectrograms. On many spectrograms H22, H23 or H24 is the last visible Balmer line in absorption. The Balmer series consists of strong emission and absorption lines. Usually the absorption components can be seen for higher series members than can the emission lines. On the two spectrograms which cover the infrared spectral region the Paschen lines are visible. The last visible Paschen lines are Pa23 on one plate (Mt. Wilson 3114) and Pa29 on the other (Mt. Wilson 3227). In the infrared spectral region the picture is greatly confused by the presence of many telluric lines.

He I: The two accessible lines of the 2^3S-n^3P series are strong in absorption and in emission. The lines of the 2^1S-n^1P series are present to $n = 8$. The leading lines of the series are moderately strong in absorption and in emission. The 2^3P-n^3S series is present to $n = 11$, the 2^1P-n^1S series to $n = 10$, the 2^3P-n^3D series to $n = 15$ and the 2^1P-n^1D series to $n = 14$. The leading lines of each series are strong in absorption and in emission. The decrease in intensity to the higher series members is strong. On most spectrograms the last visible lines of the series can be seen only in absorption.

He II: No lines of He II are present. Even at λ 4686 and λ 3203 (the 3-4 and 3-5 transitions) there is not the least indication of a spectral line being present. An emission line at λ 3204.45 must be identified as Fe III.

Li I: On Mt. Wilson spectrogram 3227 a faint absorption is seen at λ 6706.61. This feature might be identified as the first multiplet of Li I. In view of the fact that the lines at λ 6103.64 and at λ 8126.52 are absent and that the observed line is very weak and seen on one spectrogram only one must conclude that the spectrum of Li I is probably not present.

Li II: A weak emission and absorption at the position of multiplet number 1 of Li II must be identified as Fe III. In view of the high excitation potential of the Li II lines one can safely conclude that this spectrum is absent.

Be II: This spectrum is probably not present. The two lines of Be II listed in the R.M.T. were not found.

B II: This spectrum is probably not present. The line at λ 4121.95 blends with a line of He I. The line at λ 3451.41 is absent.

B III: This spectrum was looked for but not found.

C II: This spectrum is present. The lines are very weak in emission and absorption. Only the strongest lines from the study by GLAD (1952) are found.

C III: This spectrum is probably present as weak absorption lines. Only the strongest lines listed by BOCKASTEN (1955) are found. The well-known fluorescence line at λ 5696 is weak in absorption and in emission.

C IV: This spectrum is probably not present. None of the lines from the list of BOCKASTEN (1956) can be found.

N II: Many of the moderately strong lines in the spectrum of P Cygni belong to N II. Essentially all of the stronger lines listed by ERIKSSON (1957) are present in emission and absorption.

N III: Only the lines from the first two multiplets are present as weak absorption features. No emission at the λ 4634, 40, 41 multiplet can be detected. This spectrum is present.

O I: A strong absorption at λ 7769.10 with an emission at λ 7774.11 can only be identified as a blend of the first multiplet of O I. This spectrum is present. The λ 8446 multiplet lies in a heavily blended region so that it is not possible to judge its presence.

O II: This spectrum is present. All the lines listed in the R.M.T. are found. Some of the strongest lines are present as moderately strong lines in P Cygni.

O III: This spectrum is probably not present. Only the wavelengths of some of the weaker lines coincide with spectral lines in P Cygni, but in all of the cases another identification is more probable.

F II: This spectrum was searched for but no convincing coincidences were found.

F III: This spectrum was searched for but not found.

Ne I: This spectrum was looked for but due to the fact that all the stronger lines are in the infrared region of the spectrum there are some coincidences with atmospheric lines, which make a definite decision impossible. The spectrum of Ne I is possibly present.

Ne II: Most of the strongest lines coincide with weak absorption lines in the spectrum of P Cygni. In most cases, however, other identifications are also possible. The spectrum of Ne II is probably present.

Na I: This spectrum is present. The lines at λ 5890 and λ 5896 have, besides their strong interstellar components, also weak stellar absorption and emission components. No stellar components are seen at the λ 3302 doublet, but this is a much weaker multiplet.

Na II: This spectrum is possibly present. Most of the lines of this spectrum are weak. A few of the stronger lines are found, but blends with lines of other spectra may be confusing.

Mg II: Of this spectrum the doublet λ 4481 is present as a weak absorption and emission feature. The other lines of this spectrum are very weak. The spectrum of Mg II is present.

Al II: This spectrum is probably not present. Of 36 of the strongest lines only 16 coincide with spectral lines in P Cygni, but of these 13 are blended with lines of other spectra.

Al III: The wavelengths of some of the stronger lines of this spectrum coincide with weak absorptions in the spectrum of P Cygni. But multiplets numbers 3 and 5 are not found. This spectrum is possibly present.

Si II: This spectrum is present. Wavelengths and multiplet numbers were taken from MOORE (1965). The lines are weak in absorption and emission, except multiplet number 3 ($\lambda\lambda$ 4128, 4130) which is present as very weak absorption lines only, and multiplet number 2 ($\lambda\lambda$ 6347, 6371) the lines of which are moderately strong.

Si III: This spectrum is present as moderately strong absorption and weak emission lines. The wavelengths and multiplet numbers are from MOORE (1965).

Si IV: The two strong lines at λ 4088 and at λ 4116 are present as weak diffuse absorption lines. The wavelengths and multiplet numbers are from MOORE (1965). Some other lines may be present but because of blends any decision is difficult. Nevertheless the spectrum of Si IV is present.

P II: There are some coincidences but their number is not significant and in nearly all cases another identification is possible. This spectrum is probably not present.

P III: This spectrum was looked for but not found.

S II: This spectrum was looked for but not found.

S III: This spectrum is definitely present. All of the stronger lines of the R.M.T. are found in absorption, some of them are also in emission. Although the S III lines in the spectrum of P Cygni are weak, the S III spectrum is remarkably strong, when compared with other stellar spectra.

Cl II: Although some weak absorption lines correspond with wavelengths of Cl II lines no convincing series of coincidences exists. The spectrum of Cl II is probably not present.

Cl III: Of 36 lines in the R.M.T. 8 can be found, 10 others are seriously blended, while the remaining 18 are not found. This spectrum is possibly present.

Ar II: Many weak lines in the spectrum of P Cygni correspond with Ar II lines. For some of them it is the only possible identification. This spectrum is present.
Ar III: This spectrum was looked for but not found.
K I: Of the infrared doublet λ 7665, 7699 the first line blends seriously with an atmospheric line of O_2. No line is observed at the position of λ 7699. This spectrum is probably not present.
K II: This spectrum is probably not present. Of the 31 lines of this spectrum only three furnish identifications for weak absorption lines. Of the remaining 28 lines only 9 are blends, the rest of them are absent.
K III: This spectrum was looked for but not found.
Ca I: There are no indications of a stellar component of λ 4226. The spectrum of Ca I is probably not present.
Ca II: On some of the spectrograms there is a weak absorption at the expected position of a stellar component of the K line at λ 3933. A possible stellar component of λ 3968 blends with a strong absorption component of Hε. All three lines of the infrared triplet blend with Paschen lines so that their presence is difficult to judge. The spectrum of Ca II is probably present.
Ca III: Some of the strongest lines are present. The spectrum of Ca III is present.
Ti II: A search was made for the strongest lines of Ti II, but no convincing series of coincidences was found. Some of the resonance lines are present as interstellar lines.
V II: This spectrum was looked for but not found.
Cr II: This spectrum was looked for but not found.
Mn II: This spectrum was looked for but not found.
Fe II: This spectrum was looked for but not found.
Fe III: The intensities and wavelengths for this spectrum have been taken from the extensive laboratory study by GLAD (1956). Many of the stronger lines in the spectrum of P Cygni must be attributed to Fe III. This spectrum is definitely present.
Ni II: Most of the strongest lines of this spectrum coincide with weak absorption lines in the spectrum of P Cygni when an average radial velocity of -220 km/sec is taken into account. The results obtained by HERBIG (1962) were confirmed and some of the lines were also found on other spectrograms. This spectrum is present.

3.1.2. Interstellar and circumstellar lines

Besides the lines listed by HERBIG (1968) a search was made for interstellar lines arising from the lowest level of the ground term of metallic atoms and ions. The results are:
Na I: The two resonance doublets at λ 3302 and at $\lambda\lambda$ 5890, 5896 are present. The D lines are strong and show the same fine structure as the H and K lines of Ca II. The ultraviolet doublet is weak.
K I: The resonance lines at $\lambda\lambda$ 7665, 7699 were looked for. The first of these lines is masked by the atmospheric line O_2 λ 7664.87. The line at λ 7699 is not found, but also there the crowd of telluric lines makes a definite confirmation impossible. Other K I lines are not to be expected.
Ca I: The strong resonance line at λ 4226 is present as a weak interstellar feature.
Ca II: The lines at $\lambda\lambda$ 3933, 3968 are present as strong interstellar lines. On many of the spectrograms these lines show several components of various intensity. A more detailed picture is given in table 9 where the radial-velocity displacements of the different components of the strongest interstellar lines are presented.
Ti II: Of the four strongest resonance lines three are definitely present as interstellar absorption lines, while the fourth is at an unfavourable wavelength.
Fe I: Of the three lines listed by Herbig the one at λ 3719 blends with the displaced absorption component of H 14 and the one at λ 3859 blends with an absorption line of S III. The line at λ 3440 is not found. However, there is a faint but narrow absorption line at λ 3679.80 on several spectrograms which might well be due to the resonance line of Fe I at λ 3679.92. If this identification is correct this is the first time that λ 3679.92 of Fe I has been found as an interstellar line.

In addition the strongest resonance lines of Fe II, Ni I, Ti I, V I, Cr I and Mn I were looked for, but not found.

There are also some interstellar lines from molecular origin:
CH: The lines at $\lambda\lambda$ 3890, 3886 blend with two very strong lines of H and He I. The line at λ 3878 blends with a C II doublet. Only the line at λ 4300.32 is found as a sharp interstellar line. The spectrum of CH is present.
CH^+: The three strongest lines at $\lambda\lambda$ 4232, 3957 and 3745 are found. This spectrum is present.
CN: No lines are found; this spectrum is probably not present.

TABLE 4

Wavelengths and identifications

1	2	3	4	5	6	7	8
3092.53	a	2.0	1	93.41	Ar II	84	
				93.42	Si III	1	*
				93.65	Si III	1	
				94.08	Ne II	24	
3134.77	a	2.0	1	35.48	Na II	3	
36.10	e	2.0	1	36.00	S III	13	
				36.43	Fe III		*
				36.49	Fe III		
53.64	a	0	1	54.82	Ne II	14	
72.87	a	0	2	73.58	Ne II	13	
73.74	e	0	3	74.09	Fe III		*
74.80	a	0.5	1	75.99	Fe III		*
75.58	e	0.3	2	76.16	Ne II	16	
76.86	a	0.7	3	78.01	Fe III		
77.66	e	0.7	3				
84.14	a	0	1	85.13	Si III	8	*
84.68	e	0	1	85.16	S III	13	
85.98	a	4.3	4	87.74	He I	3	
87.47	e	3.3	4				
3204.45	e	0	1	04.34	Ar II	71	
				04.76	Fe III		*
04.82	a	0.3	2	06.71	N II		
				06.95	Fe III		*
10.65	a	0.3	4	12.19	Na II	4	
11.25	e	0	2				
14.25	a	0.4	4	15.63	Fe III		
15.29	e	0	3				
25.18	a	1.0	2	25.98	Na II	17	*
				26.00	Ar II	46	
29.05	as	0	2	29.19	Ti II	2	IS*
				30.16	Ne II	11	
				30.50	Si III	6	
41.87	as	1.0	3	41.98	Ti II	2	IS*
				43.34	Ne II	15	
65.23	a	2.5	4	66.89	Fe III		
66.61	e	2.3	4				
72.43	a	0	1	73.36	Ar II	71	
				73.50	O II	39	
				73.60	Fe III		*
				74.90	Ni II	1	
74.70	a	3.8	4	76.08	Fe III		*
75.84	e	2.3	4	76.26	Si III	12	
76.58	a	0	2	77.69	O II	23	
79.15	a	0	2	80.56	Fe III		
87.34	a	2.3	4	88.81	Fe III		
88.54	e	2.0	4				
90.75	a	0	2	91.47	Ar II		
91.69	e	0	2	92.04	Fe III		*
95.48	a	0	2	96.79	He I	9	
96.52	e	0	1				

1	2	3	4	5	6	7	8
3302.26	as	2.5	2	02.34	Na I	2	IS
02.86	as	0.7	3	02.94	Na I	2	IS*
				04.30	Fe III		
03.64	a	0.8	3	05.15	O II	23	
04.91	e	1.1	4	05.22	Fe III		*
06.36	a	0	2	06.60	O II	23	
07.07	e	0	2	06.99	Fe III		
				07.24	Ar II	83	
				07.30	Ni II	4	
				07.55	Fe III		*
24.03	a	0.3	3	24.57	N II		
24.99	e	0.5	1	24.87	S III	2	
28.51	a	0	3	28.73	N II		*
29.31	e	0	2	29.06	Cl III	2	
				29.20	Ne II	12	
				29.70	N II		
				29.90	Fe III		*
34.57	a	0	2	34.87	Ne II	2	
				36.12	Ne II	46	
				36.16	Cl III	6	
37.76	a	0.9	4	38.72	Fe III		
38.98	e	1.0	4	39.39	Fe III		*
				39.82	Si II	6	
46.63	a	0	2	46.99	Ca II	9	
47.24	e	0	2	47.73	Fe III		
48.00	a	0	1	50.42	Ni II	1	
71.55	a	0	2	72.68	Ca III	1	
				73.53	Fe III		
				73.98	Ni II	1	
83.65	as	3.8	4	83.76	Ti II	1	IS
95.42	a	0	3	96.70	Fe III		
96.29	e	0	3				
3404.85	a	0.7	3	06.20	Fe III		*
				07.30	Ni II	2	
06.98	a	0.5	1	07.38	O II	44	
				08.13	N II		*
23.47	a	0	1	-			
36.12	a	1.1	4	37.15	N II		
37.02	e	0.3	3				
46.37	a	0.8	4	47.59	He I	7	*
47.38	e	0	2	47.94	Si III	5.01	
				47.98	O II	27	
63.12	a	0	2	64.14	Fe III		*
				64.14	Ar II	70	
				65.62	Ni II	4	
68.71	a	0	3	70.27	Ar II		
				70.42	O II	27	
				70.81	O II	27	*
				71.35	Ni II	4	

TABLE 4 (*continued*)

1	2	3	4	5	6	7	8
3477.94	a	0	2	78.97	He I	43	*
				79.54	Si II	7.25	
95.00	a	0	1	96.27	Fe III		
97.60	a	0.7	3	98.64	He I	40	
99.25	e	1.0	2	99.49	Ar II	5	
				99.59	Fe III		*
3500.52	a	0	3	01.76	Fe III		
01.41	e	0.5	2				
09.16	a	0	1	09.78	Ar II	44	
10.05	e	0	1				
11.42	a	1.2	6	12.51	He I	38	*
12.63	e	0.5	2	13.93	Ni II	1	
14.03	a	0	1	14.39	Ar II	44	
				15.54	Fe III		*
25.87	a	0	1		-		
26.95	a	0	1	28.04	Fe III		
29.31	a	0.8	8	30.03	Cl III	10	
30.54	e	0	2	30.49	He I	36	*
35.68	a	0	1	36.82	He I	35	*
				37.75	Ca III	2	
39.03	a	0	1	39.94	Ne II	50	
42.04	a	0	1	42.90	Ne II	34	
				43.16	Ar II		
				43.25	Fe III		*
53.15	a	0.8	12	54.39	He I	34	
54.35	e	0.4	7	54.52	He I	34	
74.14	a	0.7	7	74.64	Ne II	9	*
				76.76	Ni II	4	
82.28	a	0	2		-		
83.05	a	1.0	1	84.98	C II		
84.12	e	0	1				
84.55	a	0.8	13	85.81	C II		
85.58	e	0.3	8	86.04	Fe III		
86.33	a	0.5	10	87.25	He I	31	*
87.24	e	0.4	7	87.40	He I	31	
				87.55	Fe III		
				87.66	C II		
87.63	a	0	1	88.44	Ar II	56	*
				88.92	C II		
88.57	a	0	2	89.66	C II		
90.06	e	0.9	10	89.70	Fe III		
				90.47	Si III	7	
				90.47	Ne II	32	
				90.86	C II		
91.70	a	0.5	1	93.13	Fe III		*
				93.60	N II		
99.50	a	0.6	11	00.94	Fe III		*
3600.10	as	0	1	01.51	Ar II	4	
00.82	e	1.2	12	01.62	Al III	1	
01.38	a	1.0	1	01.92	Al III	1	
02.38	e	0.5	1	02.10	Cl III	1	

1	2	3	4	5	6	7	8
3602.44	a	1.5	11	03.46	Ar II	57	
03.60	e	1.2	10	03.88	Fe III		*
				03.91	Ar II	43,68	
08.43	a	0	1	09.06	C III		
				09.10	N II		*
				09.63	C III		
10.85	a	0.8	2	11.75	Fe III		*
				11.84	Ar II	30	
				12.35	Ne II	26	
				12.35	Al III	1	
11.71	a	0.6	5	12.85	Cl III	1	
12.38	a	0.8	9	13.64	He I	6	*
13.54	e	0.5	8	13.80	Mg II	2	
15.46	a	0	1	15.86	N II		
18.23	a	0.5	1		-		
29.58	a	0	1	31.27	Na II	2	
30.96	a	0	4	32.02	S III	1	*
31.84	e	0.4	4	32.75	Ne II	33	
32.63	a	1.0	1	34.24	He I	28	*
32.97	a	1.3	14	34.37	He I	28	
34.15	e	0.9	14	34.83	Ar II	29	
48.17	a	0.4	17				
49.09	a	0	1		-		
49.42	e	0.7	13				
50.99	a	0	4	51.97	He I	27	*
51.94	e	0	2	52.12	He I	27	*
				52.67	Fe III		
54.08	a	0	1	55.11	Si III	11.03	
				55.29	Ar II	82	
56.12	e	0	1	56.05	Ar II	67	
56.69	a	0	1	56.95	Cl III	1	
57.23	e	0	1				
61.08	a	0	3	62.00	S III	6	
				62.26	H 30	6	*
63.14	a	0	4	64.09	Ne II	1	
				64.68	H 28	6	*
65.24	a	0	3	66.10	H 27	5	*
66.17	a	0	3	67.64	Fe III		
67.40	e	0	1	67.68	H 26	5	*
68.12	a	0	5	69.47	H 25	5	*
69.15	e	0	1	69.62	Ar II	42	
70.01	a	0	10	71.48	H 24	5	*
71.39	e	0	1				
71.63	a	0	2	73.26	Ar II	117	
72.35	a	0.1	10	73.76	H 23	5	*
73.76	e	0	4				
74.81	a	0.2	11	76.37	H 22	4	
75.35	a	0	4				
76.24	e	0.1	7				

TABLE 4 (*continued*)

1	2	3	4	5	6	7	8
3677.03	a	0.1	4	78.27	Ar II	42	
77.95	a	0.3	17	79.36	H 21	4	*
79.33	e	0.2	8	79.80	Ne II	41	
79.80	as	0	5	79.92	Fe I	5	IS
80.59	a	0.1	6	82.05	Cl III	1	
81.39	a	0.4	16	82.56	Ar II	29	
82.70	e	0.4	8	82.81	H 20	4	*
				83.39	Cl III	12	
83.68	a	0	2	85.40	Fe III		
84.46	a	0.4	8	86.83	H 19	4	
85.58	a	0.5	15				
86.67	e	0.5	9				
87.67	a	0.3	4		-		
89.16	a	0.1	7	90.56	Fe III		
89.84	a	0.6	10	91.56	H 18	4	
90.43	a	0.3	6				
91.52	e	0.3	13				
93.46	a	0.1	7	94.22	Ne II	1	
94.73	a	0.2	6	97.09	Ne II	41	
95.97	a	0.6	11	97.15	H 17	3	*
97.15	e	0.4	17				
98.65	a	0	3	99.37	S III		
				00.15	Fe III		*
99.66	a	0	1		-		
3701.21	as	0.1	7	01.81	Ne II	40	
				02.09	Al III	4	*
02.35	a	0.6	10	03.71	C III		
03.09	a	1.3	9	03.86	H 16	3	*
03.73	a	1.3	14	05.00	He I	25	*
04.97	e	1.6	20	05.14	He I	25	
				05.45	Cl III	1	
06.12	a	0	4	06.94	Ar II	4	
				07.34	Cl III	9	
07.53	a	0	2		-		
08.35	a	0	6	09.37	S III	1	*
				09.64	Ne II	1	
				09.90	Ar II	67	
09.69	a	0.4	7	10.42	S III	1	
10.61	a	1.0	18	11.07	Na II	3	
11.93	e	0.6	18	11.97	H 15	3	*
13.58	a	0	4	14.74	Ar II	3	
15.11	a	0	2		-		
16.84	a	0.1	10	17.78	S III	6	*
17.88	e	0	2	18.21	Ar II	131	
18.30	a	0	1		-		
19.45	a	0.7	11	20.43	Ar II	42	
20.54	a	1.1	21	20.45	Cl III	5	
21.87	e	0.9	21	21.86	Ne II	37	
				21.94	H 14	3	*
22.66	a	0.3	2		-		
24.20	a	0	3	24.51	Ar II	131	
26.48	a	0.3	19	27.08	Ne II	5	
27.42	e	0	3	27.33	O II	3	*

1	2	3	4	5	6	7	8
3731.83	a	0.8	18	32.86	He I	24	
				32.99	He I	24	
32.86	a	1.5	12	34.37	H 13	3	*
33.20	a	0.7	9	34.94	Ne II	1	
34.28	e	1.2	20				
37.08	a	0	4	37.89	Ar II	131	
40.45	a	0	1	41.69	O II	38	
45.14	as	0	3	45.30	CH^+		IS
46.62	e	0	2	46.46	Ar II	130	
				46.92	Ar II	67	
47.64	a	0.9	14	48.73	S III		
				48.81	Cl III	5	*
48.58	a	1.5	19	49.49	O II	3	
48.97	a	1.5	4	50.15	H 12	2	*
50.02	e	1.7	21	50.50	Ar II	3	
				50.74	S III	1	
51.97	a	0	2	53.17	Fe III		
54.81	a	0	2	55.61	Ca II	8	
				56.10	He I	66	*
58.11	a	0	1	58.36	Ca II	8	
64.70	a	0	3	65.27	Ar II	42	
				66.13	Ar II	29	
				66.29	Ne II	1	*
66.74	a	0.4	15		-		
67.92	a	0.7	12	68.81	He I	65	*
				69.46	Ni II	4	
68.45	a	1.4	7	70.54	Ar II	42	
69.21	a	1.7	20	70.63	H 11	2	*
70.48	e	1.8	21	71.08	N III	4	
78.43	a	0	1	78.90	S III	5	
				79.35	Cl III	8	*
83.85	a	0	3	84.89	He I	64	*
85.90	a	0	2	86.40	Ar II	3	
				87.00	Fe III		*
87.19	a	0	2	88.26	Fe III		
88.06	a	0	3	89.37	Fe III		
90.02	a	0	8	90.96	Ne II	30	
90.97	e	0.1	7	91.41	Si III	5	*
94.74	a	0.3	3	96.11	Si III	5	
95.28	a	1.2	15	96.60	Ar II	129	
96.44	a	2.2	19	97.90	H 10	2	*
97.88	e	2.1	21				
99.66	a	0	2	00.02	Ne II	39	
3804.78	a	0.3	12	05.77	He I	63	
06.12	e	0.8	20	06.30	Ne II	30	
				06.54	Si III	5	*
07.61	a	0	2	08.61	Ar II	3	
14.51	a	0	2	15.86	N II		
17.52	a	1.5	5	18.44	Ne II	39	
18.66	a	2.3	21	19.04	Ar II	129	
19.57	e	2.3	21	19.61	He I	22	*
				19.76	He I	22	

TABLE 4 (*continued*)

1	2	3	4	5	6	7	8
3820.03	a	0	1	21.68	O II	34	
20.92	a	0	2		-		
23.53	a	0	2	24.47	Cl III	9	
24.59	a	0	1	25.70	Ar II	129	
26.20	a	0	2	26.83	Ar II	54	
27.16	a	0	2	28.43	Fe III		
28.77	a	0	2	29.77	Ne II	39	
				29.79	N II		*
				30.43	Ar II	3,128	
31.11	a	0	2	31.74	C II		
				31.85	S III	5	
32.66	a	1.6	17	33.57	He I	62	
33.64	a	2.1	17	35.39	H 9	2	*
34.16	a	1.1	5	35.73	C II		
35.35	e	2.5	21				
37.35	a	0.1	14	37.80	S III	5	
				38.09	He I	61	
				38.32	S III	5	
				38.37	N II		*
39.33	a	0	2		-		
40.61	a	0	1	41.54	Ar II	54	
				42.18	N II		*
				42.46	Si III	10.03	
42.46	a	0	2	42.82	O II	12	
				43.58	O II	13	
50.75	a	0	2	51.04	O II	12	*
				51.47	O II	13	
52.12	a	0	1	53.66	Si II	1	
54.29	a	0	3	55.10	N II		
55.64	e	0.1	11	56.02	Si II	1	*
				56.06	N II		*
				56.16	O II	12	
57.99	a	0	3		-		
58.61	a	0	4		-		
59.38	a	0	2	60.64	S III	5	
60.31	a	0	2		-		
61.50	a	0	1	62.60	Si II	1	
62.92	a	0	1	63.50	O II	12	
				64.13	O II	11	
				64.45	O II	12	*
				64.68	O II	12	
65.40	a	0.3	3	67.48	He I	20	*
66.26	a	0.1	12	67.63	He I	20	
67.31	e	0.3	12				
68.36	a	0	3	68.53	Ar II	90	*
				68.87	C II		*
				69.61	Ar II	80	
70.58	a	0.3	14	71.67	C II		
71.61	e	0.2	6	71.82	He I	60	*
				72.15	Ar II	54	
76.48	a	0	2	78.03	C II		
				78.18	He I	59	*

1	2	3	4	5	6	7	8
3878.77	a	0	3	79.64	C II		*
				80.34	Ar II	54	
				80.59	C II		*
				80.84	Ar II	54	
81.45	a	0	2	82.20	O II	12	*
				82.45	O II	11	
				83.15	O II	12	
85.60	a	2.1	5	88.65	He I	2	*
86.34	a	4.4	19	89.05	H 8	2	
88.60	e	4.3	21	89.15	C III		
91.25	a	0	2	91.97	Ar II	2	
98.12	a	0	2	99.09	S III	P	
98.41	e	0	2	99.27	S III	12	
3909.96	a	0	1	10.87	Fe III		
10.88	a	0	1	11.58	Ar II	54	
				11.96	O II	17	*
				12.09	O II	17	
16.78	a	0	1		-		
18.20	a	0	3	18.98	C II		*
				19.00	N II		*
				19.00	Si II	21	
				19.29	O II	17	
19.24	a	0	2	20.37	S III	8	
20.27	e	0	1	20.69	C II		*
24.25	a	0	2	25.71	Ar II	105	
				25.87	Cl III	4	
25.34	a	0.4	20	26.53	He I	58	
26.41	e	0.3	12				
27.45	a	0	5	28.62	S III	8	*
				28.62	Ar II	10	
28.86	a	0	3		-		
29.86	a	0	1	31.24	Ar II	2	
30.52	e	0	3				
31.17	a	0	1		-		
31.53	e	0	1				
32.06	a	0	4	32.55	Ar II	90	
				33.29	S II	55	
				33.66	Ca II	1	*R
33.04	as	0	6	33.66	Ca II	1	IS*
33.25	as	0.7	6	34.41	N III	8	
33.53	as	4.0	21				
33.71	as	2.6	5				
34.00	as	2.0	1				
34.88	a	0	2	35.91	He I	57	
43.98	a	0	3	45.00	C II		*
				45.05	O II	6	
				45.20	C II		
48.73	a	0	3	49.53	C II		
50.52	a	0	2	52.06	C II		
51.74	a	0	1	52.74	Ar II	89	
53.74	e	0	2	54.33	Fe III		*
				54.37	O II	6	

TABLE 4 (*continued*)

1	2	3	4	5	6	7	8
3954.73	a	0.4	21	55.74	Si II	10	
55.63	e	0.2	14	55.85	N II		*
57.52	as	0.7	17	57.71	CH^+		IS
				58.39	Ar II	65	
58.78	a	0	2		-		
59.49	a	0	1		-		
61.44	a	0	2		-		
62.43	a	2.0	20	64.73	He I	5	
63.32	a	1.1	14				
64.45	e	2.2	21				
65.70	a	0	4	67.44	O II	22	
66.95	a	0	1	68.36	Ar II	2	
				68.47	Ca II	1	R
				68.72	Fe III		*
67.38	a	3.0	20	70.07	Hε	1	
68.13	as	2.2	5	68.47	Ca II	1	IS*
68.34	as	3.9	19	69.49	Fe III		
68.52	as	2.6	5	69.52	C II		
70.32	e	3.6	21	70.07	Hε	1	*
				70.39	C II		
72.50	a	0.2	17	73.26	O II	6	*
				73.76	C II		
81.99	a	0	4	82.72	O II	6	*
83.61	e	0	2	83.77	S III	8	
86.48	a	0	1	87.89	Fe III		
87.36	a	0	1	88.18	Ar II	65	
89.39	a	0	1		-		
90.47	a	0	3	91.50	Cl III	7	
				91.77	Si II	20	
				92.06	Ar II	2	
93.75	a	2.0	21	94.81	Ar II	89,101	
94.93	e	1.5	21	95.00	N II		*
4001.38	a	0	4	02.37	Fe III		
				03.23	Fe III		*
03.65	a	0.1	15	05.02	Fe III		
04.78	e	0.1	13				
06.63	a	0	2	07.66	Ar II	65	
				08.77	Fe III		*
08.03	a	0.9	20	09.27	He I	55	*
09.23	e	0.5	17	09.88	C II		
15.01	a	C	2	16.49	Fe III		
20.82	a	0.1	8	22.33	Fe III		
21.92	e	0	7				
22.31	a	0	1	23.99	He I	54	*
23.12	e	0	1	24.04	O II	99	
23.86	a	1.5	6	25.00	Fe III		
24.51	a	2.5	21	26.08	N II		
26.11	e	2.8	20	26.19	He I	18	*
				26.36	He I	18	
33.88	a	0	4	35.08	N II		*
				35.43	Fe III		*
				35.47	Ar II	33	
38.84	e	0	2	38.82	Ar II	2	
				39.15	Fe III		*

1	2	3	4	5	6	7	8
4040.26	a	0	6	41.31	N II		
43.80	a	0	2	44.78	N II		
47.12	a	0	2	47.51	Ar II	66	
				48.22	O II	50	
53.31	a	0	2		-		
57.83	a	0	2	59.07	Cl III	7	
64.11	a	0	2	64.45	S III		
64.98	e	0	2	65.14	Ar II	65	
				65.98	Fe III		*
67.16	a	0	3	67.94	C III		
				68.91	C III		*
69.47	a	0	2	70.26	C III		*
				70.36	Fe III		
71.50	a	0.1	8	72.01	Ar II	33	
72.57	e	0	2	72.16	O II	10	*
				72.40	Ar II	41,52	
				72.71	Si II	3.01	
				73.04	N II		*
75.06	a	0.2	10	75.45	Si II	3.01	
76.03	e	0	3	75.85	C II		*
				75.87	O II	10	*
				76.64	Ar II	52	
				76.91	N II		
77.73	a	0	1	78.86	O II	10	*
				79.60	Ar II	33	
81.19	a	0	3	81.74	Ca III	4	
				82.27	N II		*
				82.40	Ar II	8	
				82.47	Fe III		*
88.33	an	0.5	16	88.85	Si IV	1	*
				89.30	O II	48	
91.74	a	0	2	92.94	O II	10	
96.70	a	0	9	97.26	O II	20,48	
				97.31	N III	1	*
				97.58	Fe III		*
98.81	a	3.4	11	00.48	Fe III		
99.45	a	3.2	11	01.74	Hδ	1	*
4101.58	e	4.2	16	03.02	O II	20	
				03.37	N III	1	
15.49	a	0.2	16	16.10	Si IV	1	*
				16.39	Ar II	124	
				16.72	Fe III		
17.09	a	0	2	18.40	Fe III		
				18.72	Fe III		*
				18.87	Fe III		
18.59	a	0.4	6	19.22	O II	20	
19.43	a	1.0	13	19.86	Fe III		
20.58	e	0.9	15	20.28	O II	20	
				20.55	O II	20	
				20.81	He I	16	*
				20.90	Fe III		
				20.99	He I	16	
23.24	a	0	2	24.08	N II		

TABLE 4 (*continued*)

1	2	3	4	5	6	7	8
4125.01	a	0	3	26.52	Fe III		
25.60	e	0	2				
26.81	a	0	2	28.07	Si II	3	
29.61	a	0	7	30.89	Si II	3	
30.45	e	0	4				
35.05	a	0	2		-		
36.33	a	0	2	37.13	Fe III		
36.81	e	0	2	37.76	Fe III		*
41.47	a	0.9	4	42.29	S II	44	
42.37	a	1.8	14	43.52	O II	106	
43.65	e	1.1	16	43.76	He I	53	*
				43.77	O II	106	
47.37	a	0	2	48.75	Fe III		*
49.14	e	0	2	48.91	S III		
				49.65	Fe III		*
52.49	a	0	2	53.10	S II	44	
				53.11	Fe III		
				53.30	O II	19	*
55.13	a	0	2	56.11	Ar II	52	
				56.49	C III		
				56.54	O II	19	
57.42	a	0	2		-		
58.58	a	0	2		-		
60.83	a	0	2	61.35	Fe III		
62.02	a	0	2	62.70	S II	44,65	
				62.86	C III		
62.98	a	0	5	64.73	Fe III		*
64.20	e	0.1	9	64.92	Fe III		
65.33	a	0	3	66.84	Fe III		
67.86	a	0	3	68.45	Fe III		
68.84	e	0	2	68.97	He I	52	*
				68.98	Ar II		
				69.23	O II	19	
74.91	a	0	5	76.16	N II		*
				76.84	Fe III		
82.90	a	0	2	84.00	Fe III		
84.28	a	0	1	85.46	O II	38	
85.18	e	0	1				
86.74	a	0	1	86.90	C III		*
				87.14	Si II	7.17	
				88.04	Fe III		*
88.92	a	0	1	89.67	Ar II		
				89.71	S II	44,64	
				89.79	O II	36	
91.53	a	0	2	92.27	Fe III		*
				92.50	O II	42	
96.02	a	0	2	96.72	O II	42	
				97.30	Fe III		
				97.46	Fe III		
98.46	a	0	2	99.93	Ar II	124	
				99.98	N II		
				00.02	N III	6	
				00.20	Fe III		*

1	2	3	4	5	6	7	8
4201.44	a	0	3	01.99	Ar II	124	
				03.43	Ar II		
				03.83	Fe III		*
07.45	a	0	3	08.83	Fe III		
07.80	e	0	2				
10.73	a	0	2	11.65	Fe III		
				12.41	Si IV	5	*
19.40	a	0	2	19.76	Ne II	52	*
				20.92	Ne II	52	.
20.44	a	0	2	22.27	Fe III		
26.59	as	0	3	26.73	Ca I		IS
27.61	e	0	3	27.74	N II		*
				28.18	Ar II	8	
32.37	as	1.0	13	32.57	CH^+		IS*
				32.86	Si II	7.01	
36.04	a	0	2	36.91	N II		*
				37.05	N II		
				37.23	Ar II	32	
39.80	a	0	4	40.67	Fe III		*
				41.24	N II		
				41.78	N II		*
48.51	a	0	3	49.72	Fe III		
52.48	a	0.5	13	53.59	S III	4	*
53.58	e	0	5	53.74	O II	101	
				53.98	O II	101	
55.40	a	0	2		-		
65.61	a	0	4	66.53	Ar II	7	
66.91	e	0	5	67.00	C II		*
				67.26	C II		*
67.78	a	0	2		-		
71.63	a	0	1	73.41	Fe III		
73.23	a	0	2	75.19	Ar II	77	
74.66	a	0	2	75.52	O II	67	
83.45	a	0	6	84.99	S III	4	*
84.80	e	0	4	85.70	O II	78	
87.28	a	0	2	88.83	O II	54	
				89.19	Fe III		*
90.48	a	0	1	91.09	Fe III		*
				91.25	O II	55	
				91.82	C II		
4300.16	as	0	1	00.32	CH		IS
				00.66	Ar II	36,76	
				01.12	Fe III		
01.76	a	0	2	03.82	O II	53	
03.58	a	0	2	04.78	Fe III		
04.65	a	0	1	05.53	O II	55	
06.55	a	0	2	07.31	O II	53	
09.12	a	0	2	10.36	Fe III		
15.91	a	0	7	17.14	O II	2	*
17.12	e	0	3	17.19	Fe III		
				17.26	C II		
				17.65	O II	53	
18.69	a	0.3	10	19.63	O II	2	*
19.69	e	0	2	19.93	O II	61	

TABLE 4 (*continued*)

1	2	3	4	5	6	7	8
4321.10	a	0	2	21.65	O II		
				21.89	Fe III		*
				22.14	Fe III		
				22.66	Ne II	63	
24.39	a	0	2	25.56	C III		*
				25.77	O II	2	
				25.83	C II		
26.45	a	0	1	27.48	O II	41	*
27.24	e	0	2	27.89	O II	41	
27.70	as	0	1	28.18	Si IV	4	
				28.43	Fe III		*
				28.62	O II	61	
31.62	a	0	2	32.06	Ar II	1	
				32.71	S III	4	*
36.31	e	0	1	36.51	Ar II		
				36.87	O II	2	*
37.43	a	4.0	16	38.50	Si III	3	
37.86	a	2.3	3	39.78	Ne II	62	
40.35	e	4.7	15	40.30	S III	4	
				40.47	HY	1	*
44.68	a	0.1	9	45.56	O II	2	
45.40	e	0	2				
46.46	a	0	1	47.43	O II	16	
				48.11	Ar II	7	
48.50	a	0.8	13	49.43	O II	2	
49.46	e	0.2	8				
50.54	a	0.4	6	51.27	O II	16	
51.14	a	0	3	51.97	Si III	60	
52.14	e	0.5	10	52.23	Ar II	1	
				52.57	Fe III		*
				52.81	Si III	60	
62.22	e	0	2	61.87	C III		*
				62.07	Ar II	39	*
63.55	a	0	2	64.59	Al III	9	
				64.73	S III	7	
				64.74	Fe III		
66.00	a	0.6	13	66.90	O II	2	*
66.98	e	0	2	67.87	Ar II	98	
69.72	a	0	5	70.71	Fe III		*
70.85	e	0	8	70.76	Ar II	39	
				71.34	Fe III		
				71.36	Ar II	1	
71.48	a	0	2	72.31	Fe III		
				72.35	C II		
				72.49	C II		
				72.53	Fe III		
				72.81	Fe III		*
75.64	a	0	4	75.96	Ar II	17	
				76.56	C II		*
80.88	a	0.1	10	82.51	Fe III		
81.99	e	0.2	10				

1	2	3	4	5	6	7	8
4383.31	a	0	2	84.08	Ne II	60	
84.51	e	0	1	84.64	Mg II	10	
				85.00	Ne II	56	
				85.08	Ar II	98	
85.45	a	1.1	7	87.93	He I	51	*
86.30	a	2.4	14	88.02	C III		
87.81	e	1.9	16				
93.39	a	0.2	6	94.65	Ar II	87	
94.12	a	0.6	14	95.76	Fe III		*
95.37	e	1.0	15	95.95	O II	26	
4404.52	a	0	2	05.35	Si III	19	*
				05.90	Si III	19	*
				06.02	O II	26	
06.04	a	0	2	06.72	Si III	19	
11.28	a	0	2	11.51	C II		
12.75	e	0	2	12.54	Ne II	55	
				13.20	Ne II	57	*
13.87	a	0.6	16	14.91	O II	5	
14.99	e	0.4	7				
16.07	a	0.5	2	16.77	Ne II	61	
				16.98	O II	5	*
16.83	a	0.8	6		-		
17.83	a	1.4	16	18.84	S III	4	
19.15	e	1.7	16	19.23	C II		
				19.60	Fe III		*
21.68	a	0	3		-		
28.47	a	0.4	5	29.60	Ne II	74	
29.32	a	0.8	15	30.18	Ar II	7	
30.59	e	1.0	15	30.90	Ne II	56	
				31.02	Fe III		*
				31.02	Ar II	1	
36.13	a	0.3	11	37.55	He I	50	
37.33	e	0	7				
41.07	a	0	2	42.02	N II		*
				42.67	Ne II	56	
45.67	a	0.5	14	46.46	Ne II	56	
46.75	e	0.3	14	47.03	N II		*
50.34	a	0	2	52.38	O II	5	
57.25	a	0	2		-		
61.29	a	0	1	63.11	Fe III		*
				63.58	S II	43	
68.69	a	3.3	7	69.32	O II	59,94	
69.30	a	3.8	13	71.48	He I	14	*
71.31	e	3.8	15	71.52	Ne II	65	
				71.69	He I	14	
79.89	a	0.2	13	81.13	Mg II	4	
80.94	e	0.2	5	81.33	Mg II	4	
82.71	a	0	2	83.42	S II	43	
4510.59	a	0	2	10.92	N III	3	
11.57	e	0	2	11.29	Ne II	70	
				11.37	Ne II	70	
				12.54	Al III	3	

TABLE 4 (*continued*)

1	2	3	4	5	6	7	8
4513.72	a	0	2	14.80	Ne II	55	
				14.89	N III	3	*
				15.33	C III		
				15.78	C III		
18.84	a	0	1		-		
28.52	e	0	2	28.91	Al III	3	
				29.18	Al III	3	*
29.69	a	0	3	30.41	N II		*
				30.57	Ar II	35	
				30.84	N III	3	
47.88	a	0	1		-		
51.33	a	1.8	14	52.38	S II	48	
52.59	e	0.8	13	52.53	N II		
				52.62	Si III	2	*
				53.16	Ne II	55	
55.67	a	0	2		-		
59.46	a	0	2	61.03	Ar II	51	
61.62	a	0	2	62.05	Ne II	64	
66.71	a	1.6	14	67.82	Si III	2	
67.78	e	0.4	12				
73.62	a	0.9	12	74.49	Ne II	64	
74.79	e	0.1	9	74.76	Si III	2	*
80.10	a	0	2		-		
90.03	a	0	3	90.97	O II	15	
95.08	a	0	4	96.17	O II	15	
99.98	a	1.3	14	01.48	N II		
4601.26	e	1.1	14				
02.10	a	0	2		-		
05.39	a	0.5	1	07.15	N II		
05.73	a	1.3	14				
06.83	e	1.0	13				
11.43	a	0.3	2	12.89	Ne II	64	
12.46	a	0.9	13	13.67	O II	92	
13.77	e	0.9	14	13.87	N II		*
15.93	a	0	2		-		
19.88	a	1.1	14	21.28	O II	92	
21.22	e	1.0	14	21.39	N II		*
				21.42	Si II	7.05	
				21.72	Si II	7.05	
28.81	a	2.0	9	29.98	C II		
29.11	a	2.0	6	30.54	N II		*
30.38	e	1.8	14	31.24	Si IV	6	
37.74	a	0.1	10	38.28	Si III	13	
38.76	e	0	2	38.85	O II	1	*
41.14	an	1.5	14	41.81	O II	1	
42.87	e	1.2	14	41.90	N III	2	
				43.09	N II		*
44.14	a	0	2		-		
47.90	an	1.4	14	49.14	O II	1	
48.98	e	0.5	6				
49.98	a	0	7	50.84	O II	1	*
50.65	e	0	1	51.01	C III		
				51.47	C III		

1	2	3	4	5	6	7	8
4653.31	a	0	2	54.32	Si IV	7	
54.09	e	0	1	54.53	N II		*
54.97	a	0	1		-		
60.61	a	0.5	13	61.64	O II	1	
62.39	e	0	3				
75.25	a	0.3	12	76.23	O II	1	
76.14	e	0	1				
89.55	a	0	1	90.97	O II	58	
				91.47	O II	58	*
95.42	a	0	2	96.36	O II	1	
4707.86	a	0	2	09.59	N II		
				10.04	O II	24	*
10.37	a	0	4	12.07	N II		
11.18	a	1.8	14	13.14	He I	12	*
12.76	e	2.5	14	13.37	He I	12	
13.11	a	0	1		-		
14.97	a	0	3	16.23	S II	9	
16.20	e	0	2	16.65	Si III	8.09	*
57.92	a	0	1		-		
76.66	a	0	2		-		
77.51	e	0	2				
78.54	a	0.1	5	79.72	N II		
79.30	e	0	2				
79.94	a	0	2	81.19	N II		
80.90	e	0	3				
86.69	a	0	3	87.37	Fe III		
87.58	e	0	1	88.13	N II		*
4801.62	a	0	7	02.81	S III		
02.86	e	0.1	8	03.29	N II		*
08.29	a	0	2	10.31	N II		
12.51	a	0	1	13.33	Si III	9	
14.95	a	0	1	15.52	S II	9	
18.01	a	0	2		-		
19.14	a	0	1	19.72	Si III	9	
57.41	a	3.7	3	60.17	N II		
58.10	a	4.5	12	61.03	O II	57	
59.26	a	2.0	1	61.33	Hβ		R*
59.86	a	2.0	1				R
61.09	e	4.9	13				
92.87	a	0.2	3	95.11	N II		
94.46	e	0.3	5				
96.05	a	0.5	1		-		
97.00	a	0.5	1		-		
98.14	a	0	1		-		
99.01	a	0	1		-		
99.90	e	0.8	2				
4912.35	a	0.3	3	14.32	Ar II	112	
13.75	e	0	2				
19.66	a	2.4	9	21.93	He I	48	
20.15	a	1.3	2				
21.67	e	2.3	9				
23.97	a	0	1	24.60	O II	28	
				25.32	S II	7	

TABLE 4 (*continued*)

1	2	3	4	5	6	7	8
4931.66	a	0.5	1	32.80	Si II	33	
32.96	e	0.3	2	33.24	Ar II	6	
92.33	a	0.5	1	94.36	N II		
99.53	a	1.0	2	01.14	N II		
				01.48	N II		
5001.72	a	1.0	1	02.70	N II		
03.66	a	0.8	4	05.15	N II		
04.75	e	0.5	3				
05.72	a	0.5	1	07.33	N II		
06.95	e	0	1				
08.95	a	1.0	4	10.62	N II		
10.39	e	0.5	1				
12.71	a	2.6	7	15.68	He I	4	*
14.01	a	0.8	2	16.39	N II		
15.29	e	2.4	7				
41.87	a	1.0	1		-		
43.62	a	1.5	3	44.35	C II		
44.91	e	1.0	1	45.10	N II		*
45.85	a	1.0	3	47.11	C II		
47.42	e	1.3	2	47.74	He I	47	*
55.09	e	1.3	2	55.98	Si II	5	*
				56.31	Si II	5	
56.72	a	0	1		-		
61.01	a	0.5	1	62.07	Ar II	6	
				63.46	Fe III		*
71.73	a	0.5	3	73.59	N II		
73.56	e	0.7	3	73.90	Fe III		*
84.45	a	0.5	3	86.72	Fe III		
86.28	e	0.5	3				
5107.23	a	0.5	1	09.38	Fe III		
25.02	a	1.5	2	27.35	Fe III		*
27.12	e	2.0	2	27.64	Fe III		
52.43	a	0.5	1		-		
53.83	a	1.8	2	56.12	Fe III		
55.74	e	2.0	2				
91.45	a	0.3	2	92.86	Si II	23	
93.49	e	0.5	2	93.85	Fe III		
				94.07	Fe III		*
5239.94	a	0	1	43.31	Fe III		
42.65	e	0.5	1				
69.68	a	0	1	72.37	Fe III		
				72.53	C III		
75.95	e	0	1	76.48	Fe III		
81.88	e	0.5	1	82.30	Fe III		
83.20	a	0	1	84.83	Fe III		
5319.70	a	0	1	20.95	N II		
5459.19	a	0	1	60.81	Fe III		
60.40	e	0	1				
71.78	a	0	1	73.05	Si III	12.08	
				73.49	Fe III		*
				73.59	S II	6	
74.81	a	0	1	75.29	N II		
83.50	a	0	2	85.53	Fe III		*
84.97	e	0.5	2	85.74	Fe III		
93.94	a	0	2	95.67	N II		*
95.29	e	0	2	96.45	Si II	32	

1	2	3	4	5	6	7	8
5510.40	a	0	1		-		
50.62	a	0	1	51.92	N II		*
				52.67	N II		
70.65	a	0	1		-		
71.96	a	1.0	1	73.47	Fe III		
73.24	a	1.0	1	75.05	Fe III		
5614.22	a	0.5	1	16.10	Fe III		*
				16.63	S II	11'	
24.17	a	0	1	26.55	Fe III		
64.69	a	2.0	3	66.63	N II		
66.73	e	1.7	3				
74.24	a	1.5	3	75.75	Fe III		
75.68	e	0.8	2	76.02	N II		*
77.56	a	2.3	3	79.56	N II		
79.45	e	1.7	3				
84.42	a	1.5	3	86.21	N II		*
85.96	e	1.2	3	86.44	Fe III		
94.98	a	0.8	2	95.92	C III		
96.37	e	1.0	1	96.47	Al III	2	
				96.50	Si III	8.17	
5708.97	a	1.0	3	10.77	N II		
10.31	e	1.0	3				
20.97	a	0.5	2	22.46	Fe III		*
				22.65	Al III	2	
38.11	a	1.0	3	39.73	Si III	4	
39.62	e	0.3	3	40.42	Fe III		
41.58	a	0	1	44.19	Fe III		
45.31	a	0.3	3	47.30	N II		
46.90	e	0.8	2				
57.96	a	0	1				
65.70	a	1.0	1	67.44	N II		
67.03	e	1.0	1				
80.05	a	0.5	2		-		
82.80	e	0.5	1				
5802.50	a	0	1	05.16	Fe III		
04.30	e	0	1				
32.27	a	0	1	33.93	Fe III		
33.27	e	1.0	1				
36.12	a	0	1	38.04	Fe III		
38.28	e	0	1				
61.02	a	0	1		-		
72.11	a	4.0	5	75.62	He I	11	*
75.41	e	4.6	5	75.65	He I	11	*
				75.99	He I	11	*
				76.26	Fe III		
86.48	a	0.4	4	89.77	C II		
				89.95	Na I	1	R*
89.25	as	1.0	2	89.95	Na I	1	IS
89.79	as	2.8	5				
90.79	e	0	1	89.95	Na I	1	R
				91.59	C II		
				91.91	Fe III		
92.60	a	0.3	3	95.92	Na I	1	R
95.36	as	0.5	1	95.92	Na I	1	IS
95.72	as	2.4	5				

TABLE 4 (*continued*)

1	2	3	4	5	6	7	8
5896.86	e	0	1	95.92	Na I	1	R
99.69	a	0	1	00.70	Fe III		
5900.52	e	0	1	01.33	Fe III		
01.06	a	0	1		-		
04.13	a	0	1	07.21	C II		
06.14	e	0	1	07.25	Fe III		
13.45	a	0	1	14.64	C II		
14.34	e	0	1	15.22	Si II	8	
18.45	a	0	1	18.96	Fe III		
19.24	e	0.3	2	19.90	Fe III		
				20.13	Fe III		*
				20.39	Fe III		
26.17	a	0	1	27.81	N II		
28.15	a	0	1	29.69	Fe III		
28.70	e	0.3	2				
30.27	a	0.5	1	31.78	N II		
31.31	e	0	1				
40.10	a	0	1	41.65	N II		
41.40	e	1.0	1				
42.39	a	0.5	1	44.28	Fe III		
49.92	a	0	1	52.31	Fe III		*
52.81	e	1.3	2	52.39	N II		
54.09	e	0	1	53.62	Fe III		
72.59	a	0	2		-		
74.00	a	0	1	76.78	Fe III		
78.15	e	1.4	4	78.48	Fe III		
				78.93	Si II	4	
				79.32	Fe III		*
85.75	a	0	1	89.08	Fe III		
95.92	a	0	1		-		
97.39	a	0	1	99.54	Fe III		
98.81	e	0.5	3				
6002.29	a	0.5	1		-		
16.78	a	0	1		-		
20.07	a	0	1		-		
22.98	a	0	2		-		
24.91	a	0	1		-		
26.06	e	0	1				
27.18	a	0	1	28.87	Fe III		
29.03	a	0	1	32.59	Fe III		
31.79	e	0.8	4				
41.00	a	0	1	42.94	Fe III		
42.89	a	0	1		-		
6120.87	a	0	1	23.38	Ar II	102	
34.17	a	0	1	36.89	N II		
51.41	a	0	1		-		
63.23	a	0	1	65.46	Fe III		
				65.68	Fe III		*
68.17	a	0	1	69.74	Fe III		*
69.43	e	0	1	70.17	N II		
70.70	a	0	1	72.28	Ar II	102	
72.81	e	0	1	73.31	N II		*
74.61	a	0	1	76.20	Fe III		
95.88	a	0	1		-		

1	2	3	4	5	6	7	8
6223.84	a	0	2		-		
83.40	a	0.8	2	84.32	N II		
84.69	a	0	1	85.70	N II		*
				86.35	S II	9	
92.60	a	0	1	94.33	Fe III		
93.61	e	0	1	94.50	Fe III		*
95.66	as	0.5	1				
99.07	as	0.8	2				
6303.20	a	1.0	1	05.51	S II	19	
36.91	a	0	2		-		
38.49	a	0	1	40.57	N II		
40.07	e	0	1				
41.96	a	0.4	4		-		
44.32	a	0.3	2	46.67	Mg II	16	
46.17	e	1.3	4	46.86	N II		
				47.10	Si II	2	*
51.59	a	0	2	53.40	Fe III		
58.36	a	0	1		-		
62.60	a	1.0	1		-		
68.70	a	0	1	69.34	S II	19	
70.88	e	0.3	3	71.36	Si II	2	*
77.55	a	0.8	2	79.62	N II		
6400.33	a	0	1		-		
45.55	a	0	1		-		
79.89	a	1.3	4	82.05	N II		
81.78	e	1.3	3				
95.57	a	1.0	1		-		
6557.77	a	4.7	4	62.82	Hα		
58.11	a	1.0	1				
62.67	e	7.7	4				
75.32	a	0.5	3	78.05	C II		
77.30	e	0.8	3				
80.21	a	1.0	1	82.88	C II		
82.25	e	0.8	2				
99.54	a	0	2				
6607.51	a	0	2	10.57	N II		
09.68	e	0	2				
21.32	a	0	2		-		
24.62	e	0	1		-		
29.12	e	0	1	29.80	N II		
44.09	a	0	1		-		
74.34	a	3.8	4	78.15	He I	46	
77.73	e	3.8	4				
6817.81	e	0	1	18.45	Si II	7.20	
7061.19	a	3.5	2	65.19	He I	10	*
64.73	e	4.5	2	65.72	He I	10	
7112.15	a	0	1	15.63	C II		
14.02	e	0	1				
7227.23	a	0	1	31.32	C II		
30.30	e	0	1				
34.34	a	1.0	1		-		
35.86	e	1.0	1				
72.94	a	1.0	1		-		
74.09	e	0	1				

TABLE 4 (*continued*)

1	2	3	4	5	6	7	8
7277.30	a	3.5	2	81.35	He I	45	
80.62	e	3.5	2				
7318.15	a	0	1	20.14	Fe III		
44.00	a	0	2		-		
46.33	e	0	1				
7462.93	as	0	2		-		
7660.21	a	0	1		-		
61.37	e	0	1				
64.56	as	0	1	64.87	O_2	atm.	
				64.91	K I	1	IS
7706.94	a	0	1	07.43	C III		
69.10	a	1.5	2	71.95	O I	1	
74.11	e	1.5	2	74.18	O I	1	
				75.40	O I	1	
7895.45	e	0.3	2	96.37	Mg II	8	
7902.11	a	0	2		-		
8013.21	a	0.5	1	14.69	Fe III		
8233.52	a	1.0	1	35.45	Fe III		
34.75	e	0	1				
37.17	a	0	1	38.98	Fe III		
62.87	a	0	1	64.28	H	14	P35
63.91	e	0	1				
89.14	a	0	1	92.31	H	12	P29
91.48	e	0	1				
94.26	a	0	1	98.84	H	12	P28
8305.01	a	0	1	06.12	H	12	P27
11.46	a	1.0	1	14.26	H	12	P26*
				14.73	S II	12	
21.35	a	0	1	23.43	H	12	P25
22.91	e	0	1				
32.91	a	0	1	33.79	H	11	P24
42.47	a	0	1	45.55	H	11	P23
44.98	e	0	1				
56.81	a	0.3	2	59.01	H	11	P22
60.87	e	0	2	61.77	He I	68	
62.17	a	0.5	1		-		
74.63	e	0	1	74.48	H	11	P21
87.89	a	1.0	1	92.40	H	11	P20
90.97	e	0	1				
8409.12	a	1.0	2	13.32	H	10	P19
13.07	e	0.8	2				
18.16	a	1.0	1		-		
34.55	a	0.8	2	37.96	H	10	P18
37.52	e	1.0	1				
38.93	a	0.5	1		-		
40.33	e	1.0	1				
43.22	e	2.0	1		-		
44.88	e	2.0	2		-		
47.54	a	0	2		-		
50.07	e	2.0	1				
64.12	a	0.5	2	67.26	H	10	P17
66.60	e	1.0	2				
8499.03	a	1.0	2	02.49	H	10	P16
8503.06	e	1.5	2				
40.37	a	0	1	42.09	Ca II	2	
41.69	a	1.0	2	45.38	H	10	P15
45.51	e	1.0	2				
79.06	a	0.3	2		-		
82.94	e	0	2				
92.63	a	0	1	98.39	H	9	P14
94.69	a	1.5	2				
97.92	e	1.5	2				
8660.09	a	0	1	62.14	Ca II	2	
61.74	a	1.0	2	65.02	H	9	P13
64.91	e	1.5	2				
8746.65	a	0.8	2	50.48	H	9	P12
50.07	e	0.8	2				

Remarks to table 4

λ 3932.06 This weak absorption line is believed to be due principally to the stellar component of Ca II λ 3933.66.

λ 3966.95 This weak absorption line is a blend of the stellar component of Ca II λ 3968.47 and Fe III λ 3968.72.

λ 4859.26, λ 4859.86 These two lines are the only Hβ components on plate No. 3963[2]. Since they are difficult to fit in the picture presented by the other spectrograms they are mentioned separately.

λ 5886.48 This absorption line is the stellar component of Na I λ 5889.95.

λ 5890.79 This weak line is the stellar emission component of Na I λ 5889.95. Due to the presence of the strong interstellar line of Na I this emission appears to be displaced to longer wavelength.

λ 5892.60 This absorption line is the stellar component of Na I λ 5895.92.

λ 5896.86 This weak line is the stellar emission component of Na I λ 5895.95. Due to the presence of the strong interstellar line of Na I this emission appears to be displaced to longer wavelength.

3.1.3. The radial-velocity measurements

From the accurate wavelength measurements described in section 3.1 it is possible to determine the radial velocity of each measured line on all of the spectrograms. However, it appeared that the radial-velocity variations are confined to the third absorption components of the hydrogen lines. Nevertheless, because of the importance of the hydrogen and helium spectra the heliocentric radial velocities of all lines on all spectrograms are given in tables 5, 6 and 7. For the spectral lines of other elements which have constant displacements, the mean heliocentric radial velocities contain all the necessary information and are easily obtained from table 4.

The arrangement of tables 5, 6 and 7 is similar. The first column contains a number; in the case of the hydrogen lines this is the Balmer number, for the helium lines this is the multiplet number from the R.M.T. For convenience the multiplet numbers of all identified helium lines have been assembled together with the wavelengths and the transitions in table 8. The columns of tables 5, 6 and 7 are headed by the plate number and contain the heliocentric radial velocities of the different absorption components expressed in kilometers per second. In parentheses after each radial velocity is the intensity estimate according to the intensity scale of table 4 as described in section 3.1.1. Table 7 contains the hydrogen and helium lines with wavelengths greater than 5000 A. Some lines lying below 5000 A have been included, so that some cross-checking is necessary when studying these tables.

As has been pointed out by several investigators (BELOPOLSKY, 1899; FROST, 1912; KHARADZE, 1936) one must take into account several factors which tend to confuse the measured radial velocity. These will be considered in section 4.2 when the radial-velocity results will be discussed.

3.2. *The spectrophotometric measurements*

The photometric calibration of the Mount Wilson spectrograms is produced by a step slit, while that of the Victoria spectrograms is from a rotating sector. These photometric calibrations extend along the entire wavelength range of the spectrograms and allow one to find the calibration curve for each desired wavelength. At the time the Lick spectrograms were taken the step-slit calibration was not in operation so that these spectrograms were calibrated with a spot sensitometer consisting of six spots at an effective wavelength of 3700–3800 A for all of the spectrograms, except for EC-230a, for which this wavelength was 4200 A. The photometric calibration of the Haute Provence spectrograms was made using a rotating sector on a separate piece cut from the same plate as the stellar spectrogram and it was developed together with the stellar spectrogram.

In order to be able to reduce the photographic blackening to intensity a photometric calibration curve was found for each spectrogram selected for yielding line profiles. To do this, the calibration marks were recorded with the microdensitometer of the Utrecht Observatory. For each wavelength interval of about 200 A a separate calibration curve was made, each curve consisting of three independent measurements at nearly the same wavelength. Then a mean calibration curve was made for the full spectral range of each plate for which the various calibration curves did not vary significantly with wavelength.

The second part of the photometric reduction consisted of registering the stellar spectrum with a direct-intensity microphotometer. Most of the spectrograms were traced with the microphotometer of the Astronomical Institute of the University of Amsterdam. Some of the plates were traced with a new microphotometer at the Utrecht Observatory after this was installed in June 1966. On both instruments it is possible to adapt the useful intensity scale to the size of the recording paper. But with the Amsterdam instrument it is impossible to obtain a direct-intensity record for the strongest emission lines where the transmission of the photographic emulsion drops below five per cent. In that case a transmission registration was made together with the intensity tracing and the intensities of the strongest emission lines were evaluated from this transmission registration. An example of such a double registration is presented in figure 1a, in which the upper part shows a direct-intensity registration made with the Amsterdam microphotometer, the emission peaks being cut off by the instrument. The thick strongly varying line is the actual registration. The thin horizontal line and the thin slowly varying line are the continuum and line profile as drawn on the tracing. The middle part shows a transmission registration made with the same

TABLE 5

Heliocentric radial velocities of P Cygni, absorption components of H

Balmer no.	2820	2832	2877	2894	3040	3113	3466	3776	3963	8118a	8118b
4									− 90(2)		
				−166(3)			−184(3)		−127(2)		
		−239(5)	−201(–)	−234(4)		−218(4)	−234(5)	−228(5)		−198(5)	−193(5)
5	−164(3)	−180(3)					−197(1)		−197(4)		
	−236(2)	−237(1)	−197(5)	−212(4)	−209(4)	−213(4)	−233(4)	−227(4)		−191(5)	−187(5)
6	−145(3)	−171(4)					−194(0)		−179(4)	−181(5)	−193(5)
	−226(2)	−238(1)	−182(5)	−203(4)	−202(4)	−213(4)	−230(3)	−225(3)			
7	−136(2)	−176(2)							−176(3)		−169(4)
	−211(1)	−236(0)	−185(4)	−191(3)	−197(2)	−225(2½)	−226(3)	−222(2½)		−215(4)	
9	− 89(2)	− 78(½)		−101(2)	−108(1)		−110(2)				
	−126(1)	−160(1½)				−138(1)		−133(1)	−145(2)	−133(2)	−152(3)
	−222(0)	−235(0)	−173(3)	−188(3)	−196(1)	−216(2)	−228(2)	−245(1)	−236(0)		
10	−109(2)			− 96(2)	−101(2)		−105(2)				
		−159(1½)				−126(1)		−126(2)	−112(3)	−111(2)	−129(1)
	−228(0)	−251(0)	−184(2)	−192(2)		−221(1)	−228(1)	−250(1)			
11	− 88(2)	− 97(½)		− 93(2)	− 98(1)		−101(1½)			−100(1)	
	−146(1)	−157(½)				−127(1)		−117(1)	−126(2)	−161(1)	−137(1)
	−244(0)	−232(1)	−177(2)	−188(2)	−196(0)	−220(1)	−231(0)	−226(0)			
12	− 95(2)	−101(1)		− 93(2)						−107(1)	
	−146(½)	−162(1)		−140(1)	−125(1½)	−130(1½)	−115(2)	−117(1)	−120(1)		−130(1)
	−223(0)	−230(0)	−173(2)	−185(1)		−219(½)		−211(0)			
13	− 93(1)	−102(1)		− 85(1)	− 94(0)					− 93(0)	− 89(1)
	−150(0)	−167(½)				−112(1)	−118(2)	−108(½)	−118(1)	−169(0)	
			−181(2)	−195(1)*		−219(1)*	−211(1)*	−209(0)*			−201(1)*
14	− 98(1)	− 90(1)	− 93(0)	− 82(1)	−105(½)	−105(1)	− 99(1)			− 73(0)	
		−165(½)						−112(1)	−121(0)	−136(0)	−141(1)
			−183(2)	−191(0)		−204(½)		−225(0)			
15	−104(1)	− 89(1)		−100(1)			− 99(1)	−102(1)		− 88(1)	
						−145(0)					−120(1)
			−171(1)	−198(0)	−180(0)						
16	− 97(0)	− 98(0)		− 82(1)*	− 94(½)		−109(1½)	− 83(½)*			
		−161(0)									
			−191(½)			−217(0)					
17	−107(1)	− 86(0)		− 93(1)	− 85(0)		−103(½)	−104(1)			− 89(0)
	−142(0)	−160(0)	−137(0)			−128(0)					
				−191(0)						−182(0)	
18	− 91(1)	− 85(½)		− 98(0)				−107(0)			− 80(0)
		−159(0)				−137(0)	−120(½)				
			−183(½)	−179(0)				−173(0)		−178(0)	
19	−100(1)	− 94(1)	− 50(0)	− 90(1)		−103(0)	− 89(½)	− 95(0)			− 77(0)
											−171(0)
			−183(½)	−197(0)				−212(0)			
20	− 72(1)	− 86(0)		− 91(0)			−101(0)				
			−132(½)	−167(0)		−131(0)		−125(0)		−149(0)	−119(0)
		−188(0)									
21	− 96(1)	− 94(0)	− 51(0)	−100(0)			−102(0)	−106(0)			
		−160(0)	−128(½)			−124(0)					−119(0)
			−181(0)								

* H13 λ 3734 is blended with He I λ 3733; H16 λ 3704 is blended with He I λ 3705.

TABLE 5 (*continued*)

Heliocentric radial velocities of P Cygni, absorption lines of H

Balmer no.	8818	8824	EC-221	EC-228	EC-230	W1938	W1940	V1520	V1544	V1545	V1610
4											−210(4)
						−200(6)	−201(5)				−254(2)
5	−210(6)	−217(6)			−215(4)	−194(5)	−191(4)				−213(3½)
6					−145(2½)	−111(0)	−168(4)				−149(2½)
	−203(5)	−191(5)			−214(4)	−190(4)					−209(2½)
7		−184(2)		−119(3)							
	−206(2½)		−218(4)	−213(3)	−215(4)	−192(3)	−192(3½)	−210(3)	−213(2½)	−206(2½)	
9	−102(3)	− 59(2)						−103(1)			
		−177(2)	−137(3)	−135(3)	−135(3)	−114(1½)	−121(1)		−145(2)	−131(2)	−133(2)
	−210(3)		−217(2)	−214(2)	−215(2)	−188(2)	−191(2)	−208(2)	−210(1)	−207(1½)	
10	− 94(2)	− 77(2)						− 95(1)			
		−185(1)	−128(3)	−129(3)	−128(4)	−112(1½)	−114(1½)		−122(2)	−121(2)	−124(2)
	−223(1)	−227(0)	−217(1½)	−214(1)	−214(1½)	−192(1½)	−192(1½)	−214(1½)	−214(½)	−211(1)	
11	− 95(2)	− 86(1)						−100(1)			
		−181(0)	−128(3)	−130(2)	−130(3)	−117(1½)	−107(1½)		−124(2)	−123(2)	−134(2)
	−212(1)		−215(1)	−212(1)	−215(1)	−187(1½)	−193(1)	−204(1)	−206(½)	−210(1)	
12								−103(1)	− 81(1)		
	−110(1)	−110(1)	−129(2)	−128(3)	−130(3)	−115(1½)	−112(2)			−128(2)	−138(2)
			−214(1)	−217(0)	−216(0)	−191(1½)	−182(1½)	−195(½)	−183(2)	−206(½)	
13	−101(1)	− 84(0)						− 80(½)			
			−126(2)	−125(2)	−126(2)	−105(1)	−111(1½)		−108(2)	−132(2)	−128(1)
	−214(1)		−214(1)*	−215(0)*	−219(1)*	−201(1)*	−201(1½)*	−200(½)*	−228(0)*	−204(1)*	
14	−106(0)							− 97(1)			
			−129(2)	−130(2½)	−130(3)	−116(1½)	−111(1)		−116(1½)	−119(1½)	−137(1)
			−213(0)	−214(0)	−220(0)	−191(1½)	−189(1)			−214(½)	
15	− 97(0)							− 96(½)			
			−116(2)	−122(2)	−124(2)	−112(1½)	−112(1)		−119(1½)	−114(½)	−130(1)
					−214(0)	−187(1)	−189(1)			−210(0)	
16			−127(1)	−130(½)	−131(1)	−134(1)	−106(½)			−144(0)	−147(0)
			−199(0)	−212(0)	−221(0)				−203(0)		
17			−110(0)	−121(1)	−127(1)	−112(1)	−124(1)		−150(½)	−114(½)	−108(½)
						−184(½)	−208(1)			−198(0)	
18									− 88(½)		
			−131(0)	−115(½)	−136(1)	−152(1½)	−163(1)	−134(0)		−132(1)	−150(½)
			−222(0)		−216(0)						
19					− 75(0)						
			−123(0)	−123(½)	−125(1)	−115(1)	−174(1)	−119(0)	−113(½)	−107(½)	−130(0)
					−212(0)	−196(1)					
20						− 98(1)					
			−125(0)	−122(0)	−124(1)		−128(1)		−123(½)	−125(½)	−137(0)
					−219(0)	−182(½)					
21			−130(0)	−104(0)	−131(1)	−111(1)	−133(1)	−114(0)	−125(½)	−124(0)	−112(0)
					−214(0)	−203(½)					

* H13 λ 3734 is blended with He I λ 3733.

TABLE 6

Heliocentric radial velocities of P Cygni, absorption components of He I

Mult. no.	2820	2832	2877	2894	3040	3113	3466	3776	3963	8118a	8118b
3					−201(4)						
4						−174(3)					−164(2)
5	−108(2)	−100(1)	−103(3)	−102(1)	−100(½)	− 90(0)	−103(½)	−109(0)	−104(2)		− 97(1)
		−166(2)		−186(2)	−193(2)	−172(1½)	−215(2)	−204(½)	−186(2)	−160(2)	−157(2)
6	− 98(1)				− 75(1)						− 85(0)
					−204(1½)	−146(1)					−173(0)
12	−117(2)	−109(1½)		−109(2)		−132(2)		−123(1½)		−111(2)	−125(3)
		−156(1)	−150(2)	−198(0)			−149(1½)	−182(0)	−141(1)	−184(0)	
16	−100(1)	− 87(1)	− 99(1)	− 94(1)		−117(½)	−101(½)	−105(0)	−114(1)	− 85(1)	−123(1)
				−178(0)	−149(0)		−183(½)				
20	− 83(0)	− 95(0)	−116(0)			− 94(0)	− 75(0)	−120(0)		− 77(0)	−113(1)
				−173(½)							
24	−111(0)*			− 80(1)*		−104(1)*	−103(1)*	− 94(0)*			− 83(1)*
14						−118(0)		−141(3)	−146(4)		
	−142(4)	−150(4)	−171(5)	−157(4)	−174(3)	−164(3)	−183(3)	−204(3)	−193(3)	−154(4)	−152(5)
18	− 92(3)	−108(1)	−125(0)	−115(1)		−118(1)	−118(2)	−119(1½)	−120(3)	−124(3)	−131(4)
		−160(1)	−169(3½)	−176(2)	−153(3)	−172(1)	−180(1½)	−194(0)			
22	−100(3)	−106(2½)	−113(½)	−107(3)	−131(2)	−133(2)	−105(2)	−132(3)	−119(3)	− 95(1)	−121(2)
			−160(2)	−177(2)			−186(0)			−164(0)	
25	− 93(1)	− 93(1)		− 93(1)	− 90(½)		− 92(1)	−124(1)		− 85(1)	−138(1)
		−147(½)	−163(1)	−176(1)*		−146(2)		−179(½)*			
28	− 99(3)	−102(2)			− 99(1½)	−110(2)					− 99(0)
31	− 75(0)				− 71(1)	− 76(0)					− 73(0)
34	−102(1)				−107(1)	−104(1)					−117(0)
36	− 88(1)				− 92(1)	−109(1)					
38					−102(1)	−101(2)					− 94(0)
47						−105(1)					
50	−102(0)	− 94(1)	−103(0)	− 87(1)		− 91(0)				− 72(0)	− 96(0)
52				− 99(0)							− 90(0)
48						−114(2)	−103(½)	−108(3)		−119(1)	−123(2)
						−159(2)	−175(1)				
51	−109(3)	−103(2)		− 98(2)	−108(2)	−128(2)	−113(1½)	−112(2)	−114(2)	−111(3)	−116(2)
		−164(0)	−168(3)	−168(1)			−182(0)			−172(1)	
53	− 97(1½)	−126(1½)		− 87(2)	−104(1)	−103(1½)	− 94(1½)	− 96(1)	−103(2)	− 91(2)	− 92(2)
			−158(1½)	−174(0)							
55	− 53(0)		− 88(0)	− 98(2)	− 75(½)	− 82(½)	− 88(1)	− 96(½)	− 88(2)	− 71(1)	−132(1)
		−167(1)	−168(0)								
58	− 69(0)	− 84(½)	− 72(0)	− 90(1)	− 79(0)	−104(0)	− 85(½)	−128(0)	− 94(1)	− 89(0)	− 89(1)
			−152(0)								
60		− 92(0)		− 88(0)		− 78(0)	− 77(0)	−118(0)	− 98(0)	− 65(0)	−100(1)

* He I λ 3733 is blended with H13 λ 3734; He I λ 3705 is blended with H16 λ 3704.

TABLE 6 (*continued*)

Heliocentric radial velocities of P Cygni, absorption lines of He I

Mult. no.	8818	8824	EC-221	EC-228	EC-230	W1938	W1940	V1520	V1544	V1545	V1610
3			−141(5)	−144(5)						−176(3)	
4						−153(3)	−112(1½) −195(3)				−199(3)
5	−100(1½) −144(½)		−135(3)	−134(2½)	−135(3)	−114(1½) −201(1)	−123(1½) −192(1)	−108(½) −202(1)	−144(2½)	−142(2) −201(0)	−147(2)
6			−105(1) −130(1)	−131(1)	−134(½)	−104(1)	−105(1) −188(0)			−105(1)	−165(1)
12						−124(2)	−131(2)				−144(2)
16	− 96(1) −152(0)					−116(1)	−127(1½)				−139(1)
20	− 94(0)			− 85(0)	− 92(0)	−136(½)	−116(1)	− 91(0)		−109(0)	−125(0)
24	− 99(½)*		− 99(1)*	− 99(0)*	−103(1)*	− 85(1)* −100(0)	− 86(1½)* −106(0)	− 84(½)*	−112(0)	− 88(1)*	
14	−198(5)		−136(3)		−142(4)	−139(3)	−208(3)				−146(4)
18	−134(3)			−118(2½)	−137(4)	−123(2½)	−126(3)	−131(2)	−135(3)	−140(2½)	−149(3)
22	−111(3)		−124(3)	−135(4)	− 87(0) −134(3½)	−119(2)	−125(2½)	−107(2)	−131(3)	−132(3)	−142(3)
25			−110(2)	−113(1½)	−112(2)	−109(2)	−121(2)	−125(1)	−116(1½)	−135(2)	−147(1½)
28			−107(½)	−103(1)	− 88(1) −136(1)	−121(2)	−112(2) −248(0)	−130(½)	− 99(1)	−117(1)	−133(1)
31			− 88(½)	− 79(½)	− 78(1)	−101(1)	− 80(½)			− 91(0)	
34			−101(0)	− 98(1)	−100(1)	−138(1)	−110(1)		−119(1)	−111(1)	
36				− 81(½)		− 99(0)	−117(½)		− 94(1)	−119(1½)	
38						−103(1)	− 94(1)			− 81(2)	
47											−122(1)
50	− 83(0)					−102(1)	−106(½)				−129(0)
52					− 86(0)						
48						−127(3)	−133(3½)				−144(4)
51	− 98(4)				−127(3)	−113(2)	−116(2½)				−142(2½)
53	− 95(2)				− 92(3)	−111(1½)	−116(2)				−130(2)
55	− 93(2)		− 89(½)	− 99(1)	− 99(1)	−107(1½)	−112(1½)	− 87(½)		−126(1)	−120(1)
58	− 85(1)		− 95(0)	− 76(0)	− 88(0)	− 94(1)	−115(1)	− 77(½)		−108(1)	−117(0)
60	− 81(1) −126(0)			− 94(0)	− 88(0)	−108(1)	−107(1)			−110(0)	

* He I λ 3733 is blended with H13 λ 3734.

TABLE 7

Heliocentric radial velocities of P Cygni, absorption components of H and He I, $\lambda > 5000$

Line	3114	3227	3999	5388	V1551
Hα			−215(1)		−224(3)
	−229(5)	−245(10)	−246(3)		
Hβ			−215(4)		
He I 4			−177(3)		
10	−183(2)	−164(5)			
12			−136(1½)		
11	−190(4)	−198(5)	−189(3)	−164(4)	−179(4)
45	−157(3)	−177(4)			
47			−110(1)		
			−262(1½)		
46	−177(4)	−172(5)	−172(3)		−163(4)
48			−145(2½)		

instrument and at the same time. The lower part shows the resulting intensity profile scaled to a continuum intensity equal to 1.0. Filled circles are from readings of the upper registration; open circles are from readings of the middle registration after these have been converted into intensity. In all cases these emission line profiles closely match the rest of the profile that was derived with the direct-intensity recording device. Some parts of the spectrograms were registered twice on different days. It was always found that these two tracings were in good agreement, which demonstrates the reliability of the method and of the instruments used.

TABLE 8

Helium lines in the spectrum of P Cygni

	No.	Wavelength	No.	Wavelength	No.	Wavelength
n	2^3S-n^3P		2^3P-n^3S		2^1P-n^1S	
3	3	3187.743	10	7065.276	45	7281.349
4			12	4713.200	47	5047.736
5			16	4120.857	50	4437.549
6			20	3867.528	52	4168.971
7			24	3732.926		
8			27	3652.045		
n	2^1S-n^1P		2^3P-n^3D		2^1P-n^1D	
3	4	5015.675	11	5875.666	46	6678.149
4	5	3964.727	14	4471.507	48	4921.929
5	6	3613.641	18	4026.218	51	4387.928
6	7	3447.594	22	3819.637	53	4143.759
7	8	3354.550	25	3705.037	55	4009.270
8	9	3296.786	28	3634.281	58	3926.530
9			31	3587.300	60	3871.819
10			34	3554.459	62	3833.574
11			36	3530.487	63	3805.765
12			38	3512.511	64	3784.886
13			40	3498.641	65	3768.81
14			42	3487.721	66	3756.10
15			43	3478.97		
16			44	3471.80		

Most tracings have a magnification with respect to the original spectrogram of 127X. This provided a very convenient scale of wavelength on which to work. In order to draw the continuum accurately on these tracings a long ruler of 180 cm was used. The line profiles were drawn by hand on the tracing in order to correct for the graininess of the photographic emulsion. They were then reduced to an intensity of the continuum equal to one and a uniform intensity and wavelength scale. This greatly facilitated the intercomparison of the many line profiles, which will be discussed in section 5.

For the Mount Wilson 2.9 A/mm spectrograms the instrumental profile was estimated by finding the profiles of single lines in the iron arc comparison spectrum. The total width at half intensity of the instrumental profile is 0.10 A. Since the total width at half intensity of most of the spectral lines is greater than 0.8 A it was not found necessary to correct the observed profiles for instrumental broadening. The other spectrographs have comparable spectral purity.

Not all spectral lines were drawn on the standard intensity to wavelength scale; only the most important of them were chosen. These are the strongest lines of the spectra of H, He I, N II, O II, Fe III, Si III, Si IV and λ 4481 of Mg II. The equivalent widths in a spectrum with many adjoining emission and absorption lines are not easy to discuss because there will be much distortion of the line profiles. Nevertheless equivalent widths are so important in the determination of the structure of the atmosphere that their even rough determination seems fully justified. In order to resolve the overlapping emission and absorption lines it is assumed that the longward wing of the emission line and its central intensity are not distorted by the shortward absorption. Thus the initial emission line is found by simply drawing a shortward wing symmetrical to the longward wing. At the same time this procedure gives a correction for the absorption line. The whole procedure is illustrated in figure 1b, which is a demonstration of the rectification of the profile of H10 λ 3797 on plate No. 3466[1]. The thick line gives the profile from the direct-intensity registration scaled to an intensity of the continuum equal to 1.0. The thin line gives the

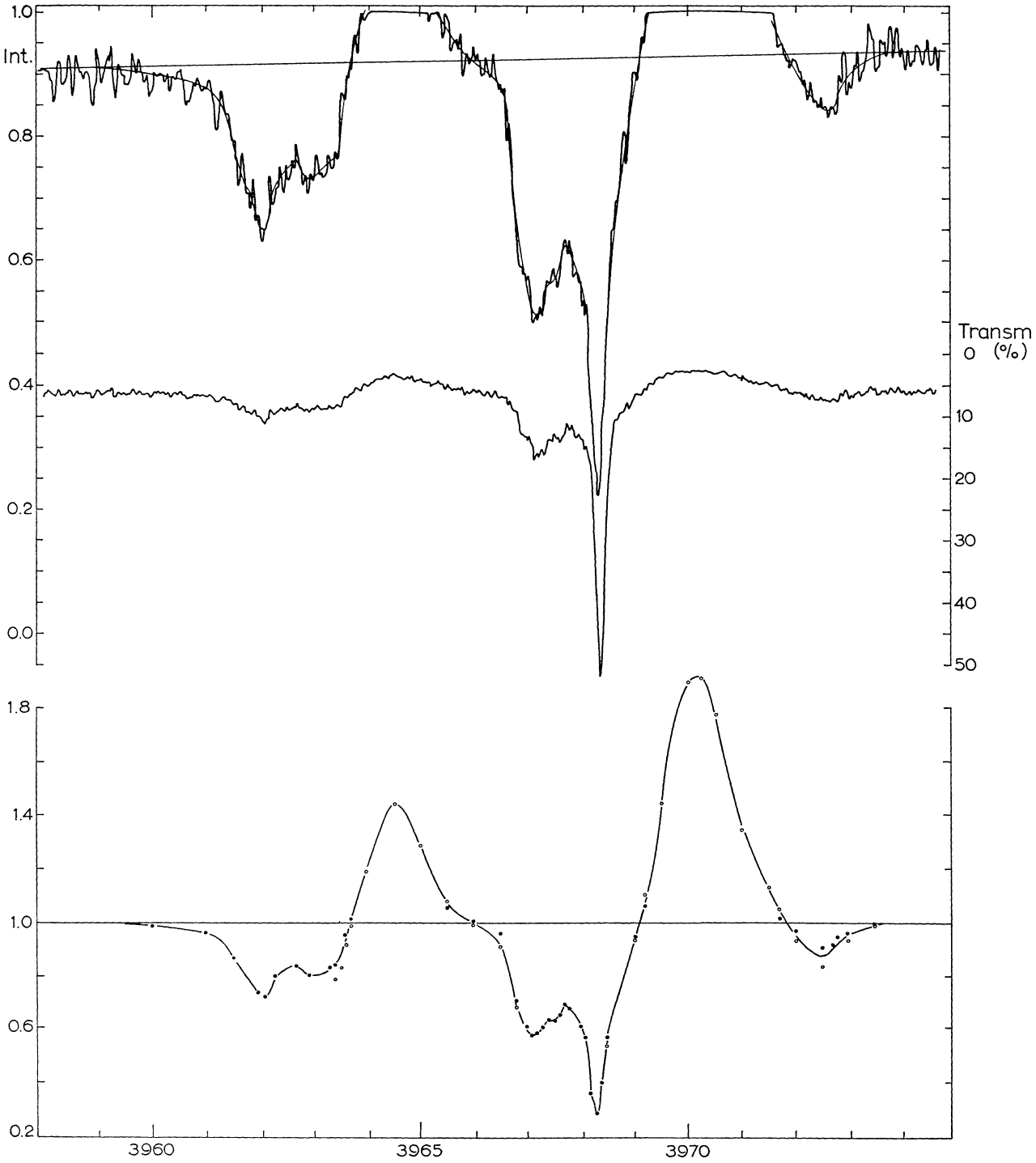

Figure 1a. Different tracings of the same wavelength region. For explanation, see text.

profile after the above mentioned correction has been made. As in many other cases there appears to be a low-velocity component which is not noticed while measuring the spectrogram with the comparator, but which shows up in the corrected profile. The radial velocity of this component is determined from the small

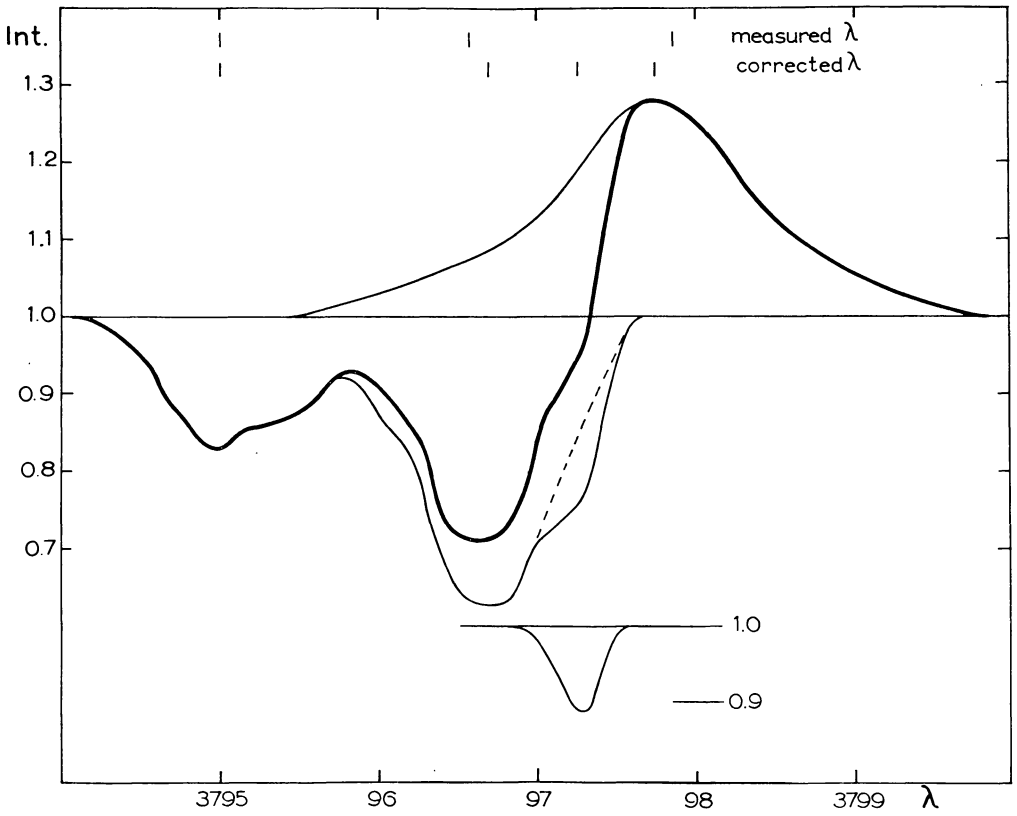

Figure 1b. Example of the rectification of a line profile. H10 λ 3797 on plate No. 3466[1]; thick line: profile from direct-intensity registration; thin line: profile corrected for overlapping of absorption and emission. In the lower part of the figure the profile is given of the low-velocity absorption component indicated by the dashed line in the upper part.

rectified profile in the lower part of the figure. Similar procedures have been adopted by other investigators (GHOBROS, 1962; LUUD, 1967a).

4. Discussion of radial velocities

4.1. *Interstellar and circumstellar lines*

Much of our present knowledge about the interstellar lines is due to the work of ADAMS (1949). He found that the strong interstellar lines of Ca II at $\lambda\lambda$ 3933 and 3968 often are composed of more than one component, which is explained by the absorption of star light in several distinct clouds. On his spectrograms of P Cygni the H and K lines of Ca II are composed of four components with radial velocities of -38, -18.6, -10.8 and -1.2 km/sec and intensities (on an arbitrary scale) of 1, 12, 12 and 2 respectively.

The radial velocities of the strongest interstellar lines studied in this investigation are presented in table 9. The average radial velocities of all interstellar lines, found from table 4, are presented in table 10. The first column gives the laboratory wavelength for each line. The other columns give the radial velocities of the various components in such a way that velocities believed to come from the same source are placed under each other in the same column. At the bottom of each column the average radial velocity of that component is given together with the residual velocity and the velocity with respect to the star itself. The residual velocities were found by correcting the measured values for reflex solar motion and the velocities relative to the star itself were found by correcting the observed radial velocities for the radial velocity -15.9 km/sec (cf. section 4.2.3) of P Cygni itself. The numbers in parentheses give the mean intensity of the line.

From a study of table 10 it is found that on many of the spectrograms of the present study Ca II components at about the same radial velocities as those observed

TABLE 9

The strongest interstellar lines in different spectra of P Cygni

λ Lab	2820	2832	2877	2894	3040	3113	3114	3227	3466
5889.95							−14.6(2)	−16.3(4)	
Na I(1)									
5895.92							−8.7(2)	−7.6(3)	
Na I(1)									
3933.66	+25.8(2)	+ 2.1(1)	− 9.5(5)	−12.6(4)	−11.4(3)	−10.7(3)			+ 2.4(2)
Ca II(1)	+17.3(5)	−10.1(4)	−51.5(0)	−47.8(0)					− 9.5(5)
	−14.3(1)	−33.8(0)							
	−21.3(1)								
3968.47	+16.8(2)	+ 1.6(2)	− 8.1(4)	−11.9(4)	− 9.0(3)	−11.3(3)			+ 2.6(2)
Ca II(1)	−14.4(4)	− 9.3(3½)							−10.7(4)
		−16.8(3)							
3383.76					− 6.6(2)				
Ti II(1)									
4232.57	−15.6(2)		−13.5(1)			−14.2(0)			−14.6(2)
CH^+									
3957.71	+12.9(1)	−14.4(2)	−13.6(1)	−15.9(2)					−14.2(½)
CH^+									

λ Lab	3776	3963	3999	5388	8118a	8118b	8818	EC-221
5889.95			−19.0(2)	− 5.8(3)				
Na I(1)				−33.4(1)				
5895.92			−17.6(2)	− 6.3(2½)				
Na I(1)				−28.6(½)				
3933.66	−12.3(4)	− 9.8(4)			−12.8(4)	−10.7(6)	−10.7(5)	− 3.4(2)
CaII(1)	−36.7(0)							−15.1(5)
	−48.3(0)							−22.7(3)
								−38.8(0)
								−51.5(0)
3968.47	−11.7(4)	−10.3(4)			− 8.3(4)	− 7.5(6)	−11.3(5)	− 5.3(2)
Ca II(1)								−15.5(5)
								−23.9(3)
3383.76								−11.7(4)
Ti II(1)								
4232.57		−14.2(2)		− 8.5(0)		−12.0(1)	−14.9(1)	
CH^+								
3957.71		−28.8(1)		−14.4(0)		− 9.8(0)	−17.4(0)	−18.9(½)
CH^+								

λ Lab	EC-228	EC-230	W1938	W1940	V1520	V1544	V1545	V1551	V1610
5889.95								− 9.7(3)	
Na I(1)								−38.2(1)	
5895.92								−12.2(2½)	
Na I(1)									
3933.66	−11.0(6)	+ 1.0(3)	− 9.6(2½)	−12.0(3)	− 9.9(3)	−11.4(3)	− 9.7(4)		− 8.6(3)
Ca II(1)	−37.1(0)	−10.8(6)							
	−48.5(0)	−34.4(0)							
		−46.7(0)							
3968.47	−10.7(5)	− 9.4(6)	− 6.7(2½)	− 7.2(3)	−11.8(3)	−11.2(2½)	−10.6(3)		−12.4(3)
Ca II(1)									
3383.76	−12.4(4)						− 7.4(1)		
Ti II(1)									
4232.57		−21.9(2)	−16.0(0)	−16.3(0)					−12.0(0)
CH^+									
3957.71	−15.1(1)	−14.4(2)	−12.5(0)	−20.4(0)	−18.9(0)		−14.4(0)		
CH^+									

TABLE 10

Mean velocities of all interstellar lines in the spectrum of P Cygni

Na I	3302.34				− 7.3(2.5)			
	3302.94				− 7.8(0)			
	5889.95				− 7.8(3.0)	−16.7(3.0)	−35.8(1.0)	
	5895.92				− 7.6(2.5)	−14.9(2.3)	−28.6(0.5)	
Ca I	4226.73					−12.6(0)		
Ca II	3933.66	+25.8(2.0)	+17.3(5.0)	+ 0.5(2.0)	−10.6(4.2)	−14.1(3.3)	−22.1(2.0)	−36.1(0)	−49.0(0)
	3968.47		+16.8(2.0)	− 0.3(2.0)	−10.0(3.8)	−15.7(4.0)	−23.9(3.0)		
	8542.09					−14.0(1.0)			
	8662.14					−13.8(1.0)			
Fe I	3679.92					−15.5(0)			
Ti II	3229.19					−13.7(0)			
	3241.98				−10.4(2.0)				
	3383.76				− 9.5(2.8)				
CH	4300.32				−11.1(0)				
CH^+	4232.57					−14.2(1.0)			
	3957.71					−14.4(0.7)			
	3745.30					−12.8(0)			
Mean radial velocity		+25.8	+17.1	+ 0.2	− 9.8	−14.4	−22.7	−36.1	−49.0
Mean residual velocity		+43.3	+34.6	+17.7	+ 7.7	+ 3.1	− 5.2	−17.6	−31.5
Mean velocity relative to star		−41.7	−33.0	−16.1	− 6.1	− 1.5	+ 6.8	+19.2	+33.1

by Adams are found, that is at −36.1, −22.7, −10.3 and +0.2 km/sec. Some spectrograms show a strong Ca II component at −14.9 km/sec. This line has to be compared with a component Adams found at a radial velocity of −13.9 km/sec which he believed to be a blend of the components at −10.8 and −18.6 km/sec. On some of the spectrograms of the highest resolution and of favourable exposure we also find components with radial velocities of −49.0, +17.1 and +25.8 km/sec. Because of the blending with the absorption components of Hε fewer components can be detected for the H line than for the K line of Ca II. The red multiplet of Ca II, strongly blended by lines of the Paschen series, has the same radial velocity as the strong blend at −14.9 km/sec.

Both Na I multiplets have a component at about −7.5 km/sec; this is somewhat smaller than the value for the strongest Ca II component. The other components of the yellow multiplet have the same radial velocities as the strong blend at −14.9 km/sec and of the component at −36.1 km/sec.

The velocities of the lines at λλ 3383 and 3241 of Ti II and the one line of CH agree well with the velocity of the strongest interstellar component of Ca II. It is therefore concluded that they are formed in the same interstellar region. The line of Ti II at λ 3229 has a different velocity but this is a weak line blended with two lines of Ne II and Si III which may easily explain a somewhat deviating velocity.

The velocities of the lines of Ca I, Fe I and CH^+ agree well with the strong Ca II blend. These lines are probably formed in both regions which contribute to the blended feature at −14.4 km/sec.

It has been argued by SCHLÜTER, SCHMIDT and STRÜMPFF (1953) that in the vicinity of a hot star surrounded by an expanding atmosphere, interstellar material will be driven away from the star by the combined action of ionization, radiation pressure and particle streaming from the expanding atmosphere. The result is that circumstellar lines should appear in the spectrum of the star and that these lines should be displaced to shorter wavelengths. The components with radial velocities relative to the star of +6.8, +19.2 and +33.1 km/sec may be considered as such circumstellar lines. It is rather curious that there also are velocities indicating a motion of circumstellar material towards the star. Such components are found at radial velocities relative to the star of −6.1, −16.1, −33.0 and −41.7 km sec. Of these the first three have about the same absolute value as the outward directed circum-

stellar components. The component at −6.1 might be explained by just another circumstellar cloud, but the other values are too high for interstellar clouds and they suggest that besides the material that is driven away from the star there also is circumstellar material falling towards the star.

The value of the radial velocity of the interstellar lines that may be expected if interstellar absorption occurs along the whole path between the Sun and P Cygni by material moving with the general galactic rotation is between 4 and 5 km/sec. This value is in satisfactory agreement with the average residual velocity of +3.1 km/sec for the strongest and most frequently observed interstellar line in the spectrum of P Cygni, so that it may be concluded that the interstellar lines of Na I, Ca I, Ca II, Fe I and CH^+ are formed over the whole distance from P Cygni to the Sun. Only the interstellar lines of CH, Ti II and one of the components of Ca II and Na I are formed in a cloud moving with a velocity which differs from the galactic rotational velocity.

4.2. *The radial velocities*

In studying the radial velocities of P Cygni it is convenient to use the following terminology for the different observed absorption components of the spectral lines. The absorption components of any spectral line showing more than one absorption component are numbered according to their relative displacement, the absorption component showing the smallest radial-velocity displacement being called the first absorption component and so on towards larger displacements. For the hydrogen lines the last observed component often is the third. For many of the helium lines and for some lines of other elements two components are observed. For the majority of the spectral lines only one component is observed.

4.2.1. The emission-line effect

As has been pointed out by various observers (BELOPOLSKY, 1899; FROST, 1912; KHARADZE, 1936) there are several factors which tend to confuse the measured radial velocities. The two most important effects are: 1. A purely photographic effect of strong emission lines widening in the emulsion during the photographic process and overlapping the absorption components. This effect can be diminished by the use of high-dispersion spectrograms. 2. The blending effect of the emission line overlapping the absorption component. The tendency is that a strong emission line will fill in a bigger part of the adjacent absorption line than does a weak emission line. The result is that the displacement of an absorption line accompanying a strong emission line will tend to be larger than the displacement of an absorption line with a weak emission component. When studying this effect it should be borne in mind that the velocity of atoms and ions in the atmosphere may depend upon the level in the atmosphere. Because in this work we are using high-dispersion spectrograms it will be assumed that the first effect has no influence. The influence of the second effect, which will be called the emission-line effect, can be estimated by studying the behaviour of lines formed at the same level in the atmosphere, and therefore with the same radial velocity, but with emission components of different intensity.

To this end a plot was made of the emission intensity of the Balmer lines with Balmer number $n \geq 9$ against the radial velocities of their different absorption components. For these lines the transition energies and the line absorption coefficients are very much the same, so that we may assume that these lines are all formed in one layer of the atmosphere and thus have the same

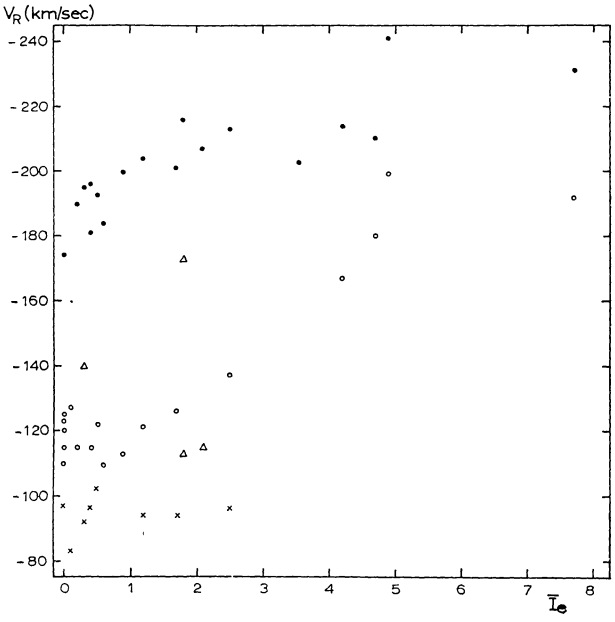

Figure 2. The radial velocities of different Balmer absorption components against the mean estimated emission intensity. Crosses: first components; open circles: second components; dots: third components; triangles: unresolved blends.

radial velocity. It is found that for the lines with Balmer number $n \geq 9$ there is only a very weak dependence of the radial velocity on the emission intensity. The picture was then extended to include also the earlier Balmer lines. The results are shown in figure 2 and will be discussed below.

In this way it is not possible to distinguish between the emission-line effect and a velocity gradient in the atmosphere. However, it is also possible to attack this problem from a different side.

When the profiles used for obtaining equivalent widths are rectified according to the procedure described in section 3.2, revised absorption profiles are found. The radial velocities of the different components of these absorption profiles are determined from the graphs and then compared with what was obtained from the measurement with the comparator. The differences between these two values of the radial velocities are always such that the corrected radial velocities have smaller absolute values, i.e. have smaller shortward displacements, in agreement with what is expected. If we now plot these radial-velocity differences against the estimated intensity, I_e, of each accompanying emission line we have a direct connection between emission intensity and radial-velocity correction. Such plots were made separately for the different absorption components of all available hydrogen and helium lines and are shown in figure 3.

If we now compare figures 2 and 3 we can draw the following conclusions. The corrections from figure 3 are much smaller than those from figure 2. This was expected because in figure 3 only the emission-line effect is present, while in figure 2 also the velocity gradient of the atmosphere plays a part. For the third absorption components there is no emission-line effect except in the case of the very strong emissions at Hα and Hβ. This can be explained when one remarks that the third absorption components are so far from their emission components that only a very strong emission has some influence. After the corrections of figure 3 have been applied to figure 2 it is found that there still is some variation of the radial velocity with the Balmer number, which clearly demonstrates the stratification of the atmosphere.

For the second absorption components there is an appreciable emission-line effect for the lines with $n \leq 10$. At $n \geq 10$, i.e. at emission intensities smaller than 2.0, the effect becomes unimportant and all lines have about the same radial velocity of -119 km/sec. The lines with $n \leq 10$ clearly show the stratification of the atmosphere, even after they have been corrected for the emission-line effect.

For the first components, figure 2 indicates that there is no variation of the radial velocity of the component with emission intensity, while figure 3 gives somewhat uncertain results. It should be noted however that a

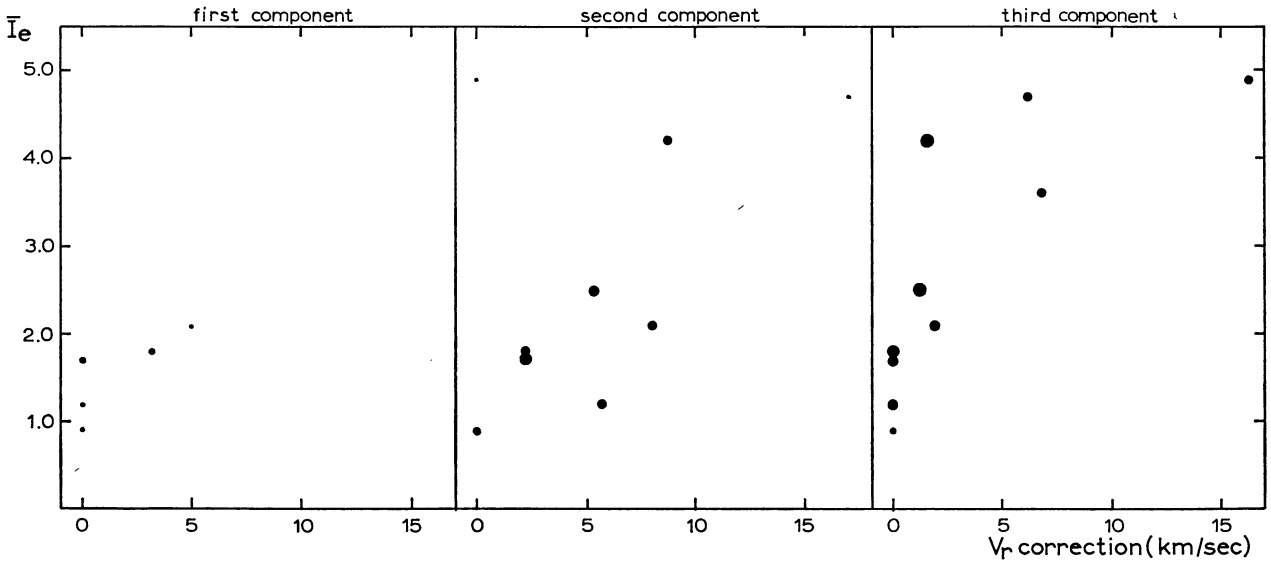

Figure 3. The radial-velocity differences (corrected — measured) against the mean estimated emission intensity showing the emission-line effect.

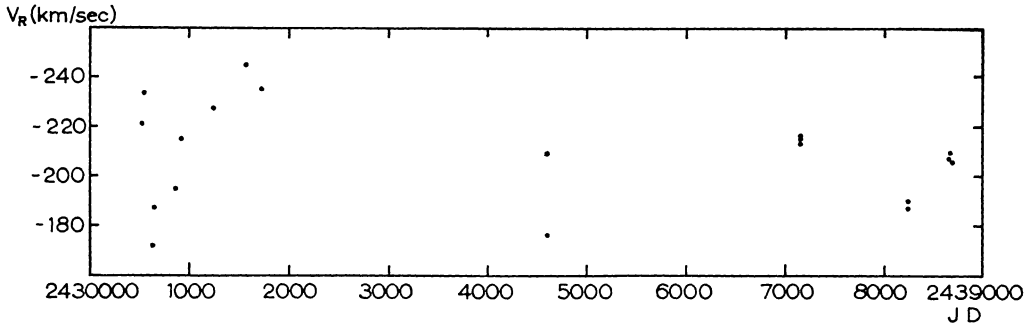

Figure 4. Radial velocity of the third absorption component of H9 λ 3835 against Julian Date.

first component at about -95 km/sec is observed only for $n \geq 9$. For these lines the emission intensity varies too little to show any appreciable effect. Also these lines are all formed rather deep in the atmosphere at higher density than the first and second components so that stratification will be difficult to find this way.

The procedure followed here with respect to the hydrogen lines serves as an illustration how the emission-line effect can be separated from the effect of a stratified atmosphere with a velocity gradient. The remark of KHARADZE (1936) that "the subsequent stage" in the correction of radial velocities in this spectrum "will

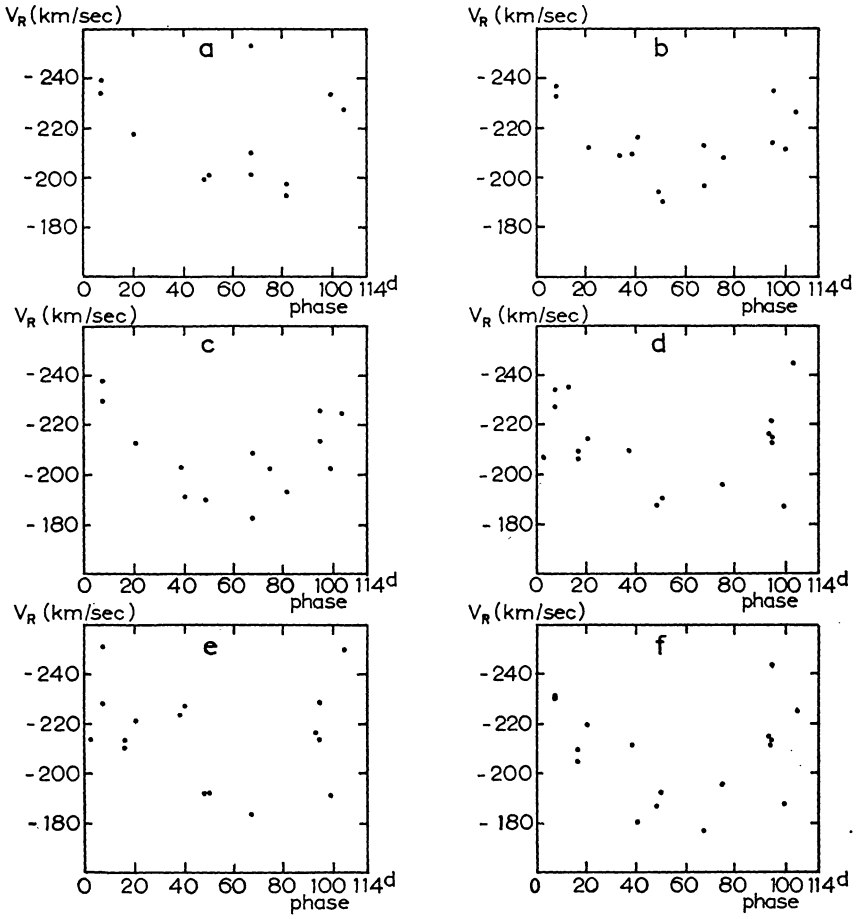

Figure 5. Radial velocity of the third absorption component of various hydrogen lines against phase in the 114-day period. a: Hβ λ 4861; b: Hγ λ 4340; c: Hδ λ 4101; d: H9 λ 3835; e: H10 λ 3797; f: H11 λ 3770.

require the accurate photometry and detailed study of the contours of the dark, as well as of the bright lines" thus proves to be fruitful.

Because the correction for the emission-line effect turns out to be small for the hydrogen lines it was not considered necessary to correct the radial velocities of tables 5, 6 and 7.

4.2.2. The radial-velocity variations

The obtained radial-velocity values can be used to investigate whether or not there is any regularity, maybe even a periodicity in the radial-velocity variations. Therefore a plot was made of the radial velocity of the third absorption component of H9 against the date of observation. This is shown in figure 4. Then this material was analysed in order to find if all points could be shifted together so as to give a smooth variation with a certain period. This technique is well-known from the analysis of variable star observations. It was found that a period of 114 days gave the best results. The radial velocities of other spectral lines were then plotted against the phase according to this 114-day period. The third absorption components of Hβ, Hγ, Hδ, H9, H10 and H11 were used; the results are shown in figure 5. It is found that all these lines show very much the same variations with corresponding phases and amplitudes. In evaluating figure 5 one should keep in mind that many of the points in the lower part of the diagram at small and at large phases are from dates on which the H lines did not show all three components. These points then are either the result of a blend between the third and second component, or they are only the second component the third being absent. In both cases these points give lower limits to the radial velocity of the third component.

Not only are the phases and amplitudes of these variations about the same, but also the mean value around which the radial velocity varies is strikingly similar for the various lines studied. If one assumes a unique relation between radial velocity and level in the stellar atmosphere, which in fact is a unique relation between radial velocity with respect to the star and the distance from the stellar surface, figure 5 could be explained in either of two ways.

1. At some high level in the atmosphere of P Cygni there is a layer which shows periodic velocity fluctuations. The velocity of that particular part of the atmosphere varies with a 114-day period between −180 and −240 km/sec.
2. The velocity field in the stellar atmosphere is fixed. The variations are introduced by variations in the opacity of the atmosphere. Sometimes we can only see as deep as the layer with a velocity of −240 km/sec and half a period later we see a deeper layer with a velocity of −180 km/sec.

Before trying to decide which of these explanations should be chosen it is investigated whether similar variations are found in the behaviour of other spectral lines.

This has been done for the second absorption component of Hδ, H9, H10 and H11; the results are shown in figure 6. It is clear that the general pattern of figure 5 is not retained. The variations are more at random. This means that these second absorption components are formed in a layer where no radial-velocity fluctuations or opacity variations of the stellar atmosphere occur.

The same results are obtained for the radial velocities of the helium lines. From different series the best measured lines were selected and their radial velocities plotted against the phase in the 114-day period in figure 7. The lines at λλ 3964, 4471, 4387 and 4120 are used for this purpose. There are no indications of variations in that part of the atmosphere where these helium lines are formed. The second components of the lines at λ 4387 and at λ 4120 have radial velocities of about −180 km/sec and this value is well below the value found in the case of the varying velocity of the third components of the hydrogen lines. For the two other lines, λλ 3964 and 4471, the second components have radial velocities of nearly −200 km/sec. This value is about equal to the velocity minima of the third components of the hydrogen lines. That no variations are found in the case of λ 4471 may be due to the small number of measured second components. For λ 3964 the mean velocity of the second component is −193 km/sec, whereas the third hydrogen absorption component with smallest radial velocity, H11, still gives −208 km/sec. The conclusion is that even the radial velocity of λ 3964 is not subject to variations because this line is formed just below the layer of the atmosphere in which the variations occur.

4.2.3. Stratification of the atmosphere

The Balmer progression. – For each measured spec-

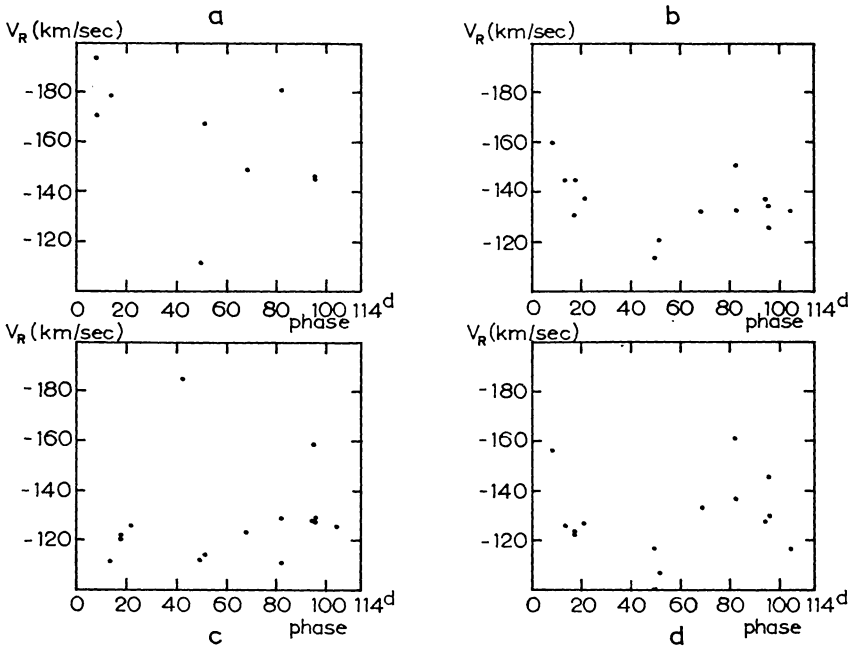

Figure 6. Radial velocity of the second absorption component of various hydrogen lines against phase in the 114-day period. a: Hδ λ 4101; b: H9 λ 3835; c: H10 λ 3797; d: H11 λ 3770.

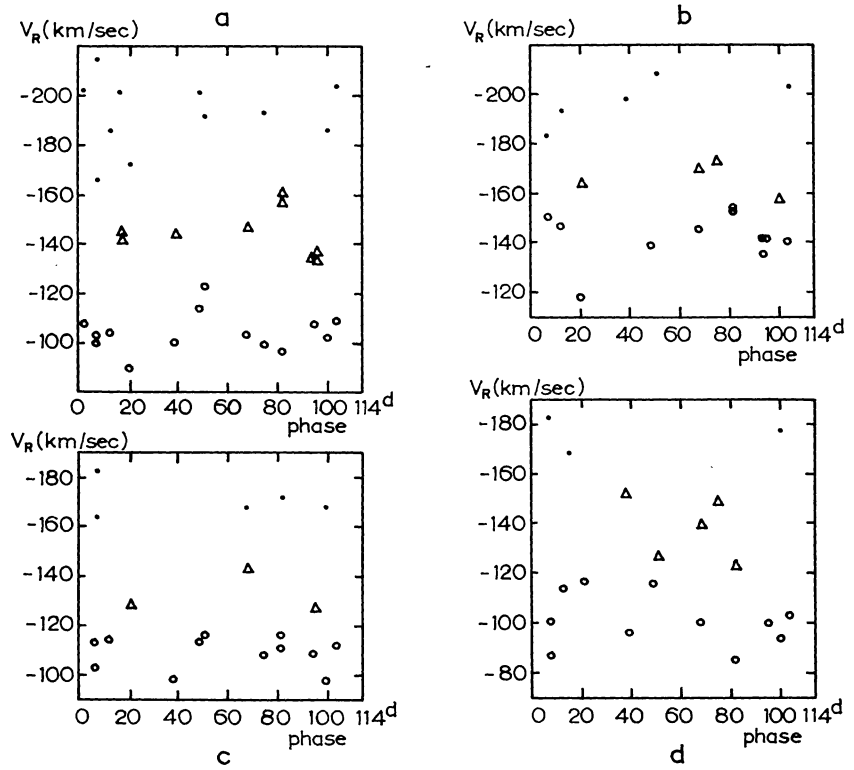

Figure 7. Radial velocity of different absorption components of some He I lines against phase in the 114-day period. a: λ 3964; b: λ 4471; c: λ 4387; d: λ 4120. Open circles: first components; dots: second components; triangles: unresolved first and second components.

trogram the radial velocities of the absorption components of the Balmer lines after correction for the emission-line effect were plotted against their Balmer number. Some typical results are shown in figure 8. The slope of the line is known as the Balmer progression. In all cases the values for H8 were omitted because this line is seriously blended with He I λ 3888 and the results can not be trusted. All three absorption components are not visible on all of the spectrograms as can be seen from the figure for plate No. 2894. This spectrogram, together with No. 2877, shows another peculiarity: the third components of the earliest Balmer lines give a slope which is quite different from that obtained from the other series members. Apart from these two exceptions all the other spectrograms show Balmer progressions of their various absorption components which are all very close to zero.

Some insight into a possible distribution of velocity and density in the extended atmosphere of P Cygni can be obtained by postulating that a given central depth of an absorption line in the spectrum corresponds to a certain value of the monochromatic optical depth. Consider for example the first components of the Balmer lines. These components have about the same central absorption for all lines from Hγ to H20, thus by hypothesis they have about the same monochromatic optical depth at the line centre. Since the absorption coefficients of the different lines of the Balmer series do not have the same value but are largest for the earliest members, the geometrical depth of formation of a late Balmer member must be larger than that of an early member. Since all the Balmer lines show the same radial velocity one must conclude that the different Balmer lines are formed over a range of depth in the atmosphere of P Cygni which has a constant radial velocity.

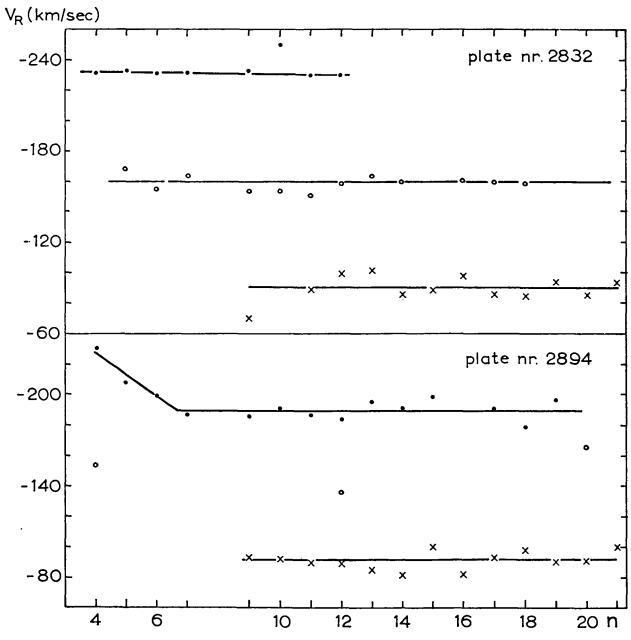

Figure 8. Radial velocity of hydrogen absorption lines against upper quantum number n for two spectrograms. Meaning of symbols as in figure 2.

The dependence of the radial velocity upon the excitation. – It is known (BEALS, 1935; STRUVE, 1935; KHARADZE, 1936) that the radial velocity from absorption lines arising from levels of different excitation potential varies in P Cygni; lines of low excitation generally indicate higher velocities of expansion than those of high excitation. When investigating this type of correlation it is necessary first to correct for the emission-line effect (cf. section 4.2.1). One may use either the average radial velocities determined from unblended absorption lines only, or the average radial velocities determined from all available absorption lines irrespective of their blending. The average radial velocities obtained in these two ways are called V_A and V_A' respectively. In the second case it is assumed that the different influences of many blends will be negligible in the average. The validity of this assumption was checked by noting for each spectrum whether the majority of the blends are on the longward side of the lines concerned or on their shortward side. The results are that in the case of longward blends both the absorption and the emission radial velocities have more positive values than for unblended lines; in the case of shortward blends both these velocities are more negative. This is exactly what one would expect and it suggests that one can use blended lines to enlarge the number of lines studied and improve the quality of the results, provided one uses the velocity difference between absorption and emission radial velocity. In a radially expanding transparent envelope the emission-line radial velocities give the radial velocity of the star itself. Using the velocity difference this means that all absorption velocities are referred to the average stellar velocity as indicated by the displacements of the emission lines of the element concerned.

As a measure of the level of excitation neither the ionization potential nor the excitation potential should

be used. Using the ionization potential of a certain ion as an index of the level of excitation does not take account of the sometimes rather different values of the excitation potential for the lines of two spectra with nearly the same ionization potential. Similarly using the excitation potential of a certain level within a certain ion completely ignores the differences in ionization energy between the several ions of the same element.

A more suitable procedure can be found by considering the quantity $N_{r,s}$, the number of atoms or ions in the proper level for absorbing the lines of a given multiplet. The value of $N_{r,s}$ can be related to the number of atoms, N_0, and the number of ions, N_r, by the relation

$$N_{r,s} = N_0 \cdot \frac{N_r}{N_0} \cdot \frac{N_{r,s}}{N_r}. \qquad (1)$$

Assuming the validity of Saha's law for the ratio N_r/N_0 and Boltzmann's law for $N_{r,s}/N_r$ and taking natural logarithms, we obtain $\log N_{r,s}$ = constant − (I.P.+ E.P.)/kT, where T is the temperature in the layer, assumed to be constant. These considerations suggest that the sum of the ionization and excitation potentials should be used as a measure for the excitation and called the total excitation energy of the line. For an absorption multiplet of Fe III, for example, the total excitation energy is the sum of the ionization potentials of Fe I and Fe II and the excitation potential of the lower level of the multiplet in the Fe^{++} ion. Since for many multiplets only very few lines could be measured, the use of total excitation energies for each multiplet leads to results which scatter widely. Therefore an average total excitation energy for all multiplets of a given spectrum was used.

The results shown in figure 9 reveal more detail than was suspected by others (Beals, 1935; Struve, 1935; Kharadze, 1936) who were able to draw only a single curve relating velocity of expansion to energy of excitation. The curve splits near an excitation energy of about 35 eV. Towards lower excitation energies there are three different curves. Each of these curves is connected with one of the three observed absorption components of the hydrogen lines. The two lower curves merge into each other at about 35 eV. At the excitation energy of the He I lines, about 21 eV, these two curves still are so close to each other that the two components will not be seen separately. The observed "second" component of

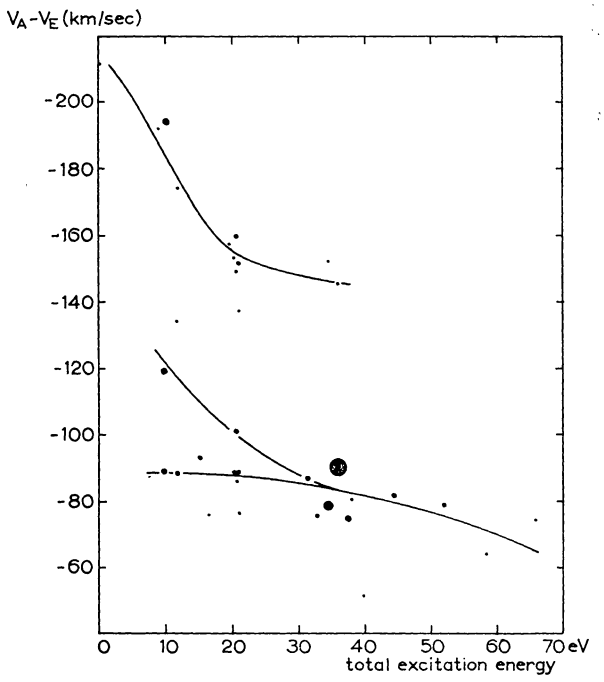

Figure 9. Radial velocity of absorption lines against total excitation energy. The size of the points is a measure for their weight.

the He I lines is found to fit nicely on the upper curve which contains the third hydrogen absorption and the "second" components of some of the strongest lines of N II and Fe III.

This result now should be compared with the results on the Balmer progression. In comparing the radial velocities of different Balmer lines the most important parameter for obtaining any knowledge about the velocity field in the atmosphere is the monochromatic optical depth in the centre of the line, τ_0. For the Balmer lines we have

$$\tau_0 = \kappa_0 N_{0.2} H, \qquad (2)$$

where the absorption coefficient in the centre of the line is

$$\kappa_0 = \frac{\sqrt{\pi} \cdot e^2 \cdot \lambda \cdot f}{m \cdot v \cdot c}. \qquad (3)$$

The oscillator strength f varies by a factor of 30 between Hβ and H10. At the same time λ decreases by a factor of 1.3, so that in going from Hβ to H10 κ_0 decreases by a factor of 40. Now, since the optical depth in Hβ and H10 has to be the same at the level where the major contribution to the line absorption is

made, the geometrical depth H in the case of Hβ has only $1/40\times$ the value of H in the case of H10 if the density ρ remains constant. This implies that for these lines to be formed in layers of the atmosphere having the same radial velocity, ρ has to be fairly high, or else that the velocity remains unchanged over long path lengths.

When lines of different elements are intercompared, the relative abundances of the elements enter the picture. If we make the reasonable assumption that gf between multiplets of different elements varies by a factor of 10, and that there is a variation in N(abundance) of a factor of 10^4 (hydrogen compared with metals), the decrease in τ_0 from a strong line of an abundant element to a weak line of a less abundant element may amount to a factor of about 10^5. Since in this case κ_0 varies only with a factor of 10, a decrease with a factor of 10^5 in τ_0 means an increase with a factor of 10^4 in H. We therefore conclude that the Balmer lines all originate in about the same level of the atmosphere and that the lines of various elements are formed over a considerably greater depth of atmosphere. This interpretation makes compatible the facts that the Balmer progression is zero whereas a dependence of the radial velocity on the total excitation energy is observed for weaker lines.

When the emission radial velocities, V_E determined from all available emission radial-velocity measurements irrespective of blends are plotted against excitation energy, the result shown in figure 10 is obtained. The mean radial velocity from all these lines is -15.9 km/sec. A few points fall rather far outside the general range of velocities. The point at 0 eV is from the sodium D lines whose weak emission is displaced to longer wavelengths due to the influence of the strong interstellar absorption. The other high points are from Cl III and C III. The presence of Cl III is a bit doubtful and the C III value is from one blended line only. All other spectra give values in the range between -5 and -35 km/sec.

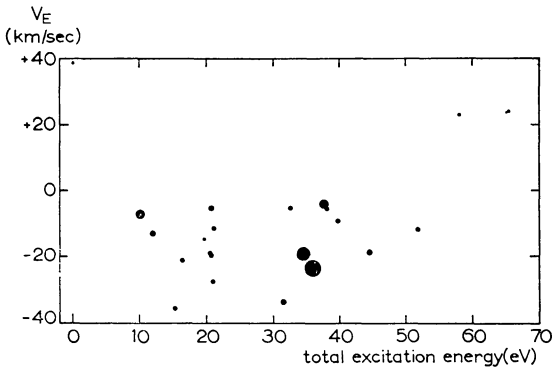

Figure 10. Radial velocity of emission lines against total excitation energy. The size of the points is a measure for their weight.

Although the individual spectra give somewhat divergent results the mean radial velocity gives a fair estimate of the radial velocity of the star itself. This value is in reasonable agreement with the results of BARBIER (1962) for 70 O- and B-type stars in the region of IC 4996. Her values spread between -25 and $+20$ km/sec with an average radial velocity of -9.0 km/sec. Also this value is quite close to the radial velocity of -10 km/sec that one expects for a star at the distance of P Cygni with no other motion than that of the general galactic rotation.

4.3. *Rotation and turbulence*

From figure 9 it can be inferred that almost all spectral lines are formed in the extended atmosphere, though at different heights. If we want to determine the rotational velocity of the star itself we should find lines that are formed mainly in the stellar photosphere. These are the lines of high excitation energy such as the Si IV doublet at λ 4088 and λ 4116.

Using the method described by UNSÖLD (1955, section 124) and assuming a value of 0.4 for the limb-darkening coefficient in this region of the spectrum (GRYGAR, 1965), we find an upper limit for the observed rotational velocity of P Cygni, $v \sin i < 80$ km/sec. This value is in good agreement with the average value, between 70 and 90 km/sec, for the O9-B1 supergiants (BOYARCHUK and KOPYLOV, 1958).

It has been remarked by HUANG and STRUVE (1951) that in the spectra of the early-type supergiants it is extremely difficult to judge whether line broadening is due to rotation or to macroturbulence. VAN DEN HEUVEL (1965) has concluded from statistical arguments that macroturbulence is the chief line-broadening mechanism in early-type supergiants, whereas ROSENDHAL (1968) has found from a consideration of the evolutionary effects that rotation is as important as macroturbulence in the early B-type supergiants. Therefore, not too much weight should be placed on the above-derived value of $v \sin i$; it only is a confirmation of the normal supergiant character of P Cygni.

TABLE 11

Mean equivalent widths of hydrogen lines in the spectrum of P Cygni

Line	First component (mA)	Second component (mA)	Third component (mA)	Total absorption (mA)	Total emission (mA)	log $N_{0,2}H$
Hβ	388 2	690 2	712 2	1790 2	9669 3	13.86
Hγ	349 1	904 2	330 2	1583 2	5552 3	14.33
Hδ	172 6	562 6	359 6	1093 6	2179 7	14.52
Hε					1148 4	— blend Ca II
H8				1362 2	2564 2	15.11 blend He I
H9	85 6	365 6	315 6	765 6	474 6	15.04
H10	71 5	380 5	120 5	571 5	420 5	15.07
H11	65 5	304 5	178 5	547 5	352 5	15.19
H12	56 5	351 5	120 5	527 5	246 5	15.30
H13	33 3	252 3	176 2	461 3	190 3	15.35
H14	46 2	209 2	88 2	343 2	201 2	15.33
H15	15 2	151 2	70 2	236 2	134 2	15.26

5. Discussion of spectrophotometric measurements

5.1. *The equivalent widths*

All equivalent widths were corrected for overlapping when necessary according to the procedure explained in section 3.2. The mean equivalent widths of the hydrogen lines are given in table 11. On the plots of the rectified line profiles each absorption component was drawn as well as possible, and the equivalent width of each component as well as that of the total line was measured. A similar procedure has been followed for the helium lines. However, not all of the helium lines could be separated into two components, in which case only the total absorption was measured. The helium equivalent widths are presented in table 12. Table 13 contains information concerning other spectral lines, most of which have only one component. In each of these tables the number following each equivalent width gives the number of spectrograms included in the mean value.

The mean equivalent widths of tables 11, 12 and 13 do not give information on variations of the equivalent

TABLE 12

Mean equivalent widths of helium lines in the spectrum of P Cygni

Transition	Line	First component (mA)	Second component (mA)	Total absorption (mA)	Total emission (mA)	log NH
2^1S-n^1P	3964	169 5	406 5	575 6	394 6	13.91
	3613			208 1	127 1	13.88
2^3P-n^3S	4713	241 6	121 6	362 6	642 6	14.21
	4120	200 7	90 7	290 7	216 7	14.59
	3867			143 2	26 2	14.63
2^3P-n^3D	4471	282 5	734 5	1016 6	1934 6	13.67
	4026	507 4	298 4	805 4	858 4	14.08
	3819	296 5	322 5	618 6	298 6	14.29
	3705				186 2	
	3554			176 1	25 1	14.59
	3530			103 1	13 1	14.50
2^1P-n^1S	4437			160 2	8 2	14.43
	4168			99 1	0 1	14.63
2^1P-n^1D	4921			526 1	392 1	13.31
	4387	321 6	241 6	562 6	276 6	13.89
	4143	235 7	211 7	446 7	82 7	14.12
	4009	169 6	142 6	311 6	31 6	14.24
	3926			205 1	23 1	14.31

TABLE 13

Mean equivalent widths of lines of N II, O II, Mg II, Si III, Si IV and Fe III in the spectrum of P Cygni

Line	Absorption (mA)	Emission (mA)	Line	Absorption (mA)	Emission (mA)
N II 3955	119 3	35 3	Si III 4552	446 3	39 3
3995	461 5	96 5	4567	402 4	11 4
4447	87 2	50 2	4574	250 3	5 3
4601	220 4	112 4			
4607	226 4	71 4	Si IV 4088	280 5	0 5
4613	161 4	58 4	4116	259 5	0 5
4621	190 4	103 4			
4630	462 5	275 5	Fe III 4005	92 3	44 3
			4419	495 4	457 4
O II 3973	87 4	0 4	4431	264 4	154 4
4345	95 1	0 1			
4366	140 2	0 2	O II+		
4414	163 3	0 3	Si III 4253	218 2	0 2
4661	204 4	24 4			
			Fe III		
Mg II 4481	125 4	17 4	+O II 4395	244 4	186 4

widths of individual lines. However, it is necessary to investigate whether such variations exist. The most obvious period for such variations would be 114 days, as for the radial-velocity variations. Since the radial-velocity variations are limited to the outermost shell of the atmosphere one would expect a variation of the line intensities to be present only in the lines that are formed in this outermost shell. Unfortunately the spectrograms most suitable for measuring equivalent widths are very badly spread in phase according to this 114-day period, all clustering around $\varphi = 10^{d}$ and $\varphi = 100^{d}$ with only one exception. Therefore, the only meaningful figures that can be obtained come from consideration of the spread of the individual equivalent widths around their mean value. Table 14 gives the individual equivalent-width determinations for each of the absorption components and for the emission component of some representative hydrogen and helium lines. The mean values from these measurements are also given. It should be noted that spectrograms 2820 and 3776 were recorded and reduced twice so that the equivalent widths from these two plates enter into the mean value with double weight. The second last column gives the standard deviation in the mean equivalent width

$$\sigma = \left\{\frac{1}{n}\sum (W_i - \overline{W})^2\right\}^{\frac{1}{2}}, \qquad (4)$$

where n is the number of individual equivalent widths W_i, and $\overline{W}$ the tabulated mean equivalent width. All equivalent widths in table 14 are given in milliångströms.

On the other hand it is also possible to estimate the probable error of one observation from the quality of the material and from a comparison of the equivalent widths that were determined from the two sets of recordings of spectrograms 2820 and 3776.

The statistical accuracy of equivalent-width measurements on high-dispersion spectrograms has been studied by UNDERHILL and DE GROOT (1965). From their table 3 a figure of 15 per cent is obtained for the average probable error in the measurement of an equivalent width below 80 mA and 6 per cent for equivalent widths between 81 and 100 mA. Even though in a spectrum like that of P Cygni it is quite difficult to determine the level of the continuum within an accuracy of a few per cent due to the presence of both emission and absorption lines, it is found from a comparison of spectrograms 2820 and 3776 that for lines with an equivalent width below 300 mA the average probable error is nearly 15 per cent. This value corresponds to a standard deviation, σ_E, of 18 per cent. For the stronger lines the proportional probable error is less; for these lines an equivalent-width measurement has an accuracy of about 50 mA. These values of σ_E for each line are presented

TABLE 14

Equivalent widths of some selected lines

Line	Component	2820	2832	2877	2894	3466	3776	221	228	230	Mean W	σ	σ_E
Hδ	W_{A1}	259	265		125	174	} 331			133	172	69	31
	W_{A2}	549	732		} 965	463				763	562	172	50
	W_{A3}	177	156			479	499			488	359	144	50
	W_E	1840	2598		1914	2036	2516			2172	2179	312	50
H9	W_{A1}				35	79	116	81	106	95	85	26	15
	W_{A2}				168	396	303	475	348	500	365	109	50
	W_{A3}				535	297	235	294	206	325	315	106	50
	W_E				423	436	569	415	406	596	474	78	50
H12	W_{A1}				40	64	37	20		117	56	34	10
	W_{A2}				254	400	339	386		376	351	52	50
	W_{A3}				200	142	88	78		92	120	46	22
	W_E				204	270	201	275		282	246	36	44
He I 3964	W_{A1}		300			244	219	34	} 408	50	169	105	30
	W_{A2}		289			430	191	571		547	406	147	50
	W_E		502			382	424	313	337	407	394	63	50
4120	W_{A1}	232	221			215	159			185	200	27	36
	W_{A2}	57	101			110	80			144	90	30	16
	W_E	224	217			166	210			330	216	56	39
4471	W_{A1}	346	203	133	380					} 1039	282	103	50
	W_{A2}	733	816	746	645						734	61	50
	W_E	2015	2550	768	2271					1983	1934	757	50
4387	W_{A1}	477	307	101	340					223	321	129	50
	W_{A2}	106	228	267	257					480	241	121	43
	W_E	344	308	113	194					351	276	94	50

in the last column of table 14. It is seen immediately that in practically all cases all calculated deviations σ are definitely larger than the deviations σ_E expected for constant quantities.

The conclusion is that nearly all spectral lines of P Cygni vary in some irregular way over a range of about 30 per cent. This value is in good agreement with the value derived by LUUD (1967a) from a comparison between his measurements and those of BEALS (1950). A comparison may also be made with the results of KUPO (1955) and of DOLIDZE (1958). They found that in 1951 and 1952 P Cygni showed irregular spectrophotometric variations coincident with the light and colour variations of the star.

The equivalent widths of tables 11, 12 and 13 have been compared with the results obtained for other stars of similar spectral type in order to get an idea about the exact spectral type of the P Cygni absorption spectrum. For this comparison the following stars were chosen: ε Ori, B0Ia (WILSON, 1958; LAMERS, 1968); ρ Leo, B1Ib (UNDERHILL, 1948; WRIGHT *et al.*, 1964); ζ Per and 139 Tau, B1Ib (GRAVES, BAKER and WILSON, 1955); κ Cas, B1Ia (WILSON, 1956); HD 190603, B1.5Ia (BUTLER and SEDDON, 1958); χ^2 Ori, B2Ia (UNDERHILL, 1948; BUTLER and SEDDON, 1958); HD 14143, B2Ia (BUTLER and SEDDON, 1958). The results are shown in figures 11a to h. Each section of figure 11 contains the corrected equivalent widths of absorption lines in P Cygni as ordinate and the corresponding values for another star as abscissa. An inspection of these figures leads to the conclusion that the comparisons with the B2Ia stars HD 14143 and χ^2 Ori and with $\frac{1}{2}$ (χ^2 Ori + ε Ori), about B1Ia, give the best agreement. To judge whether κ Cas, B1Ia, or HD 190603, B1.5Ia, yields the better agreement with P Cygni is rather difficult owing to the small amount of data. The agreement with the three stars of luminosity class Ib is less good (especially at the higher values of the equivalent width which have not been included in the picture for technical reasons). Therefore, since each star should be considered as an individual object and since complete agreement between two early-type stars will probably never be found, the spectral type of P Cygni, according to the absorption lines, is between B1 and B2. The luminosity

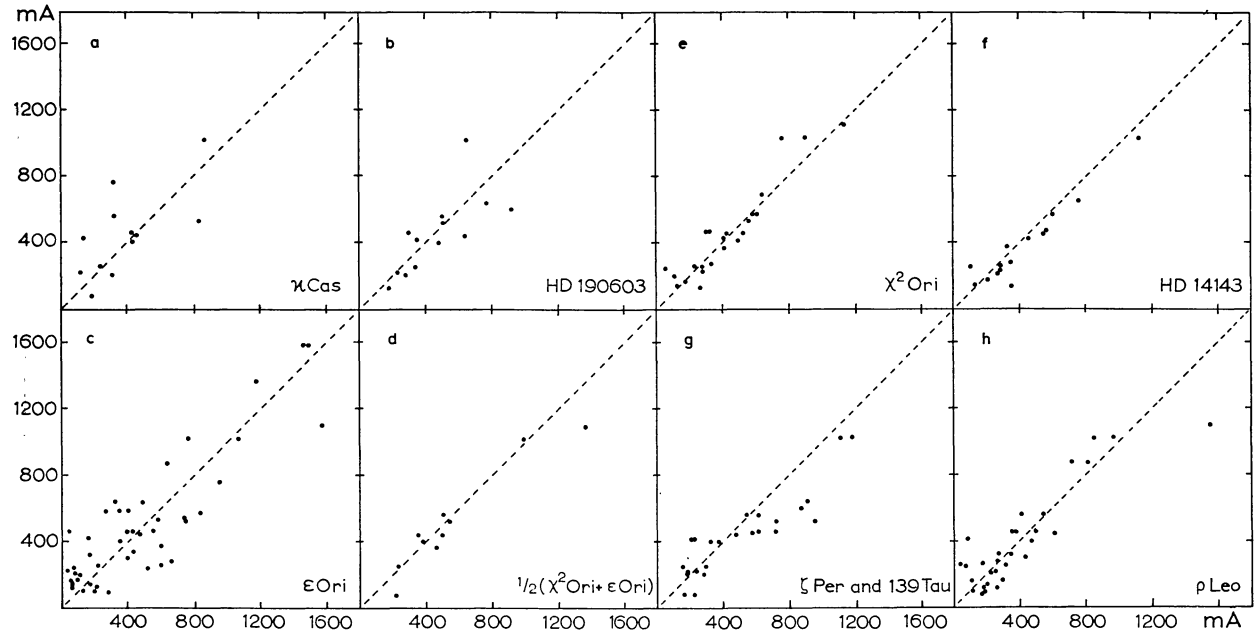

Figure 11. Comparison of equivalent-width measurements with those for other stars of similar spectral type. a: κ Cas, B1Ia; b: HD 190603, B1.5Ia; c: ε Ori, B0Ia; d: ½ (χ^2 Ori+ε Ori); e: χ^2 Ori, B2Ia; f: HD 14143, B2Ia; g: ζ Per and 139 Tau, B1Ib; h: ρ Leo, B1Ib.

class can be estimated rather accurately as Ia since the absorption spectrum very closely resembles that of a normal Ia supergiant and not that of a Ib supergiant.

A comparison may be made with the equivalent widths found by other authors at different epochs. LUUD (1967a, b) has published equivalent widths for the major lines in the spectrum of P Cygni for the years 1964, 1965 and 1966 separately. He indicates equivalent

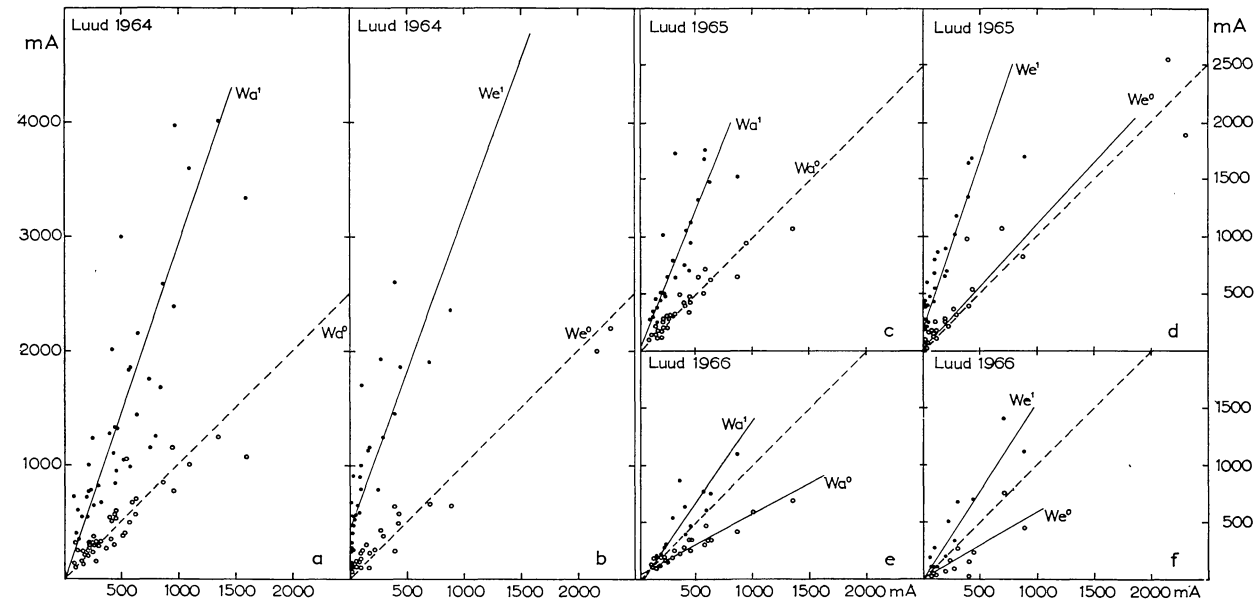

Figure 12. Comparison of equivalent-width measurements with those of LUUD (1967a, b). a: absorption lines during 1964; b: emission lines during 1964; c: absorption lines during 1965; d: emission lines during 1965; e: absorption lines during 1966; f: emission lines during 1966. Dots represent values corrected for overlapping of absorption and emission; open circles represent uncorrected values. Abscissae: corrected values from the present study.

widths measured on a microphotometer tracing uncorrected for overlapping of absorption and emission lines with the superscript 0; a superscript 1 is used for values corrected for the effect of overlapping. Luud's corrected and uncorrected absorption and emission equivalent widths are shown plotted against our corrected equivalent widths in figure 12 for each of the years mentioned. In each section of figure 12 open circles represent the comparison with uncorrected values, dots with corrected values of the equivalent widths. The relations between the equivalent widths are represented also by the straight lines drawn in each figure. The dotted lines have a slope of 45 degrees. The slopes of the full-drawn straight lines are presented in table 15. In this table W_a^0, W_a^1, W_e^0 and W_e^1 refer to equivalent widths of other authors and W_A and W_E to our equivalent widths.

From table 15 it can be seen that for 1964 and 1965

TABLE 15

A comparison with equivalent widths measured by other authors

	Luud			Beals	Ghobros
	1964	1965	1966	1929–1950	1951
W_a^0/W_A	1.00	1.00	0.53	1.00	2.17
W_a^1/W_A	2.91	2.45	1.45		
W_a^1/W_a^0	2.91	2.45	2.74		
W_e^0/W_E	1.00	1.09	0.60	1.26	0.65
W_e^1/W_E	2.71	2.90	1.55		
W_e^1/W_e^0	2.71	2.76	2.58		
Dispersion (A/mm)	1.5–36	15–36	15–36	7–15	42 at Hγ

Luud's uncorrected values are about the same as our corrected values, while his corrected values are two to three times larger than the present values. Luud's 1966 values are much reduced but the ratio between corrected and uncorrected values still has the same high value. The large emission equivalent widths obtained by Luud can be explained by his choice of correction procedure. He assumes that the first absorption component is formed in the stellar photosphere and therefore he has to magnify his emission profiles very much in order to centre them at this supposed zero wavelength. However, the radial-velocity measurements show unambiguously that the emission lines are at the undisplaced position. Therefore the corrections must be much smaller and as a result more accurate. For instance, from a comparison of our figure 1b with Luud's figure 3 (LUUD, 1967a) it can be seen that both the equivalent width and the central intensity of Luud's emission lines are rather ill-defined compared to ours.

A comparison has also been made with the results published by BEALS (1950) based on spectrograms obtained between 1929 and 1950. The results are presented in figures 13a, b and in the fifth column of table 15. Beals did not correct his equivalent widths for the effect of overlapping so that in fact his results should be compared with our uncorrected values. Since the mean ratios of corrected equivalent widths to uncorrected widths are 1.08 for the absorption lines and 1.27 for the emission lines of this study, the equivalent widths of Beals are about a factor 1.5 larger than the present ones.

Finally we compare our results with those of GHOBROS (1962) (see figure 13c and the sixth column of table 15). Ghobros measured some hydrogen and helium lines only. The results of the comparison are rather strange. Ghobros' absorption equivalent widths are a factor two larger and his emission equivalent widths about a factor two smaller than the present values.

The differences between the equivalent widths just

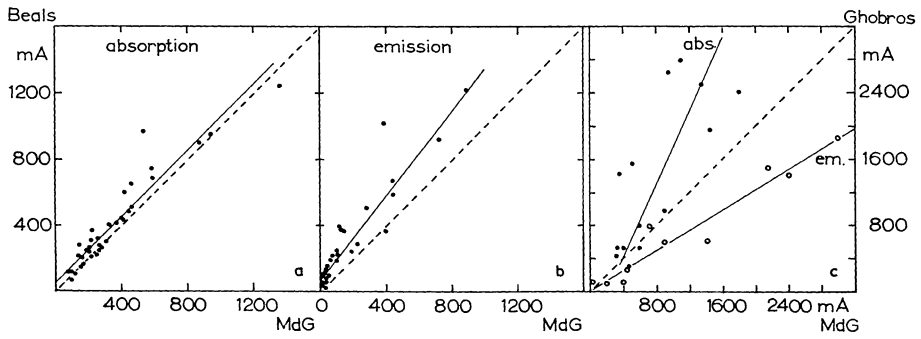

Figure 13. Comparison of equivalent-width measurements with those of BEALS (1950) and of GHOBROS (1962). a: absorption lines, Beals; b: emission lines, Beals; c: absorption lines (dots) and emission lines (open circles), Ghobros.

mentioned were also noticed by LUUD (1967a) who explained them by real variations of the spectrum of P Cygni. This explanation seems rather plausible in the case of our comparison with Beals but the results of Ghobros are strongly suspected to have suffered from a too high continuum, probably as a result of underestimating the emission intensities of lines other than hydrogen and helium.

Although from the equivalent widths it is impossible to determine whether the variations of the absorption-line intensities show a certain period, some conclusion can be drawn on the basis of the estimated intensities of table 5. When the ratios of the absorption intensities of the third and second components of the hydrogen lines are plotted against the phases according to the 114-day period the results suggest a quite regular variation with strong third components at phases around 57 days and strong second components at phases around 0 days. This observation will be discussed in section 7. Before a definitive answer can be given to the question whether there are spectral variations for all spectral features in common and whether these variations are periodic, more spectrograms more closely spaced in time will have to be analysed in a more uniform way than has been done so far.

5.2. *The atmospheric parameters*

The electron density, N_e, can be estimated from the chief quantum number of the last visible Balmer line, n_m, with the aid of the well-known Inglis-Teller formula,

$$\log N_e = 23.26 - 7.5 \log n_m. \qquad (5)$$

Here the spectrum of P Cygni presents a complication since the Balmer lines consist of more than one absorption component. In this way it is not possible to determine the electron density of each of the shells separately because the lines of each shell become invisible not only through their relative proximity but also because there always is the component of the other shell in between making the lines look broader and confusing the picture. Therefore our estimate of n_m will be a lower limit and consequently the derived value of N_e will be an upper limit.

In order to find n_m a plot was made of $\log n$ against $\log (1-R_c)$ for the third absorption components and for the blend of the first and second absorption components of the hydrogen lines. Here n is the Balmer number and R_c the central absorption in units of the intensity of the continuum at the wavelength of a Balmer line. It is found that for $n \geq 9$ both relations are straight lines which permit a simple extrapolation to $\log (1-R_c) = 0$. The two components yield the same value $n = 25$ and $\log N_e = 12.76$. Apart from the fact that this is an upper limit of N_e it also should be kept in mind that this is an average value of N_e over all spectrograms measured for line profiles. For instance, on plate EC-221 the Balmer lines are visible to $n = 30$ whereas on most of the other spectrograms the last visible Balmer line has $n = 24$. Thus it seems that this average value of N_e should be interpreted as the normal electron density, whereas a value $\log N_e = 12.18$ as derived from $n_m = 30$ would represent rather extreme conditions.

It is assumed that each of the shells in the extended atmosphere of P Cygni is a uniform layer which can be described by one value of the temperature and the particle density. This assumption permits the calculation of the total number of excited hydrogen atoms along the line of sight in each of the shells, $N_{0,2}H$. The method used is the one given by UNSÖLD (1955, section 118E) which makes use of the relation

$$W_\lambda = \frac{\pi e^2 \lambda^2}{mc^2} N_{0,2} H f, \qquad (6)$$

which is equivalent with the logarithmic expression

$$\log N_{0,2}H = 12.06 + \log W_\lambda - 2 \log \lambda - \log f. \qquad (7)$$

Values of $\log N_{0,2}H$ have been calculated for all available absorption equivalent widths of the hydrogen lines and are shown plotted against the Balmer number n in figure 14. The different absorption components yield very similar curves. The low values of $\log N_{0,2}H$ for low n are caused by the fact that in the earliest Balmer members the shells are optically thick so that not all hydrogen atoms present contribute to the formation of the spectral line. For the highest Balmer numbers the lines begin to overlap and the continuum is suppressed so that a too small value of the equivalent width is measured. If this overlapping did not occur the limiting value of $\log N_{0,2}H$ for large n would be the true value since it corresponds to an optically thin layer for which the formula given above is correct. In the present case since the curve bends down beyond

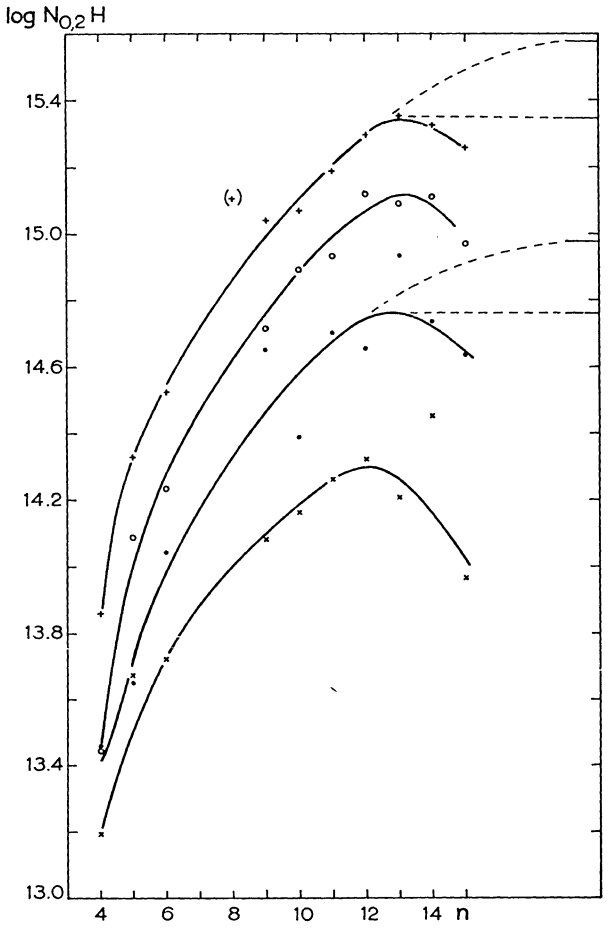

Figure 14. Log $N_{0,2}H$ against Balmer number n. Plus signs are for total absorptions, other symbols as in figure 2. Dashes in upper right part are from table 16.

$n = 13$, the maximum values reached are taken to be the true values of log $N_{0,2}H$, but they are in fact only lower limits.

According to the method given by Unsöld the value of $N_{0,2}H$ can also be determined from the Balmer jump,

$$D = \log I_{3647+} - \log I_{3647-}. \qquad (8)$$

However, the Balmer jump which has been determined by several investigators (BARBIER and CHALONGE, 1941; BARBIER *et al.*, 1947; CHALONGE and DIVAN, 1952) proves to be so near to 0.0 mag that it cannot be used to determine the corresponding apparent absorption

$$R = 1 - 10^{-D}. \qquad (9)$$

An inverse procedure is followed here. From the adopted value of log $N_{0,2}H$ for the total hydrogen absorption the expected intensity change at the Balmer jump is calculated from the expression

$$R = 1.38 \times 10^{-17} \times N_{0,2}H. \qquad (10)$$

With log $N_{0,2}H = 15.35$ this gives $R = 0.03$ and $D = 0.01$ mag. This value of D is smaller than the accuracy with which D can be determined from good observations, confirming the observed value of $D = 0.0$ mag. It is now possible to start from the calculated value of D and by taking the finite optical thickness of the layer into account to find another value of $N_{0,2}H$. In this case we do not use the value of R derived from formula (9) but the quantity κ defined by

$$\frac{1}{R} = \frac{1}{\kappa} + \frac{1}{R_c}, \qquad (11)$$

where R_c is the limiting central absorption for Balmer lines near the Balmer jump. From a plot of R_c against λ the value of $R_c = 0.07$ is found. With the aid of formulas (11) and (10) this gives log $N_{0,2}H = 15.58$. This value has been inserted as a horizontal dash in the upper right corner of figure 14. The dotted line shows that without any difficulty the value log $N_{0,2}H = 15.58$ can be reconciled with the values of log $N_{0,2}H$ calculated from the equivalent widths.

This procedure, of course, can also be applied to the log $N_{0,2}H$ values for the individual shells. Since, however, the first and the second absorption components of the Balmer lines are so close together that it is not easy to separate them, only two values of $N_{0,2}H$ are calculated in this way: one for the first and second absorption together and one for the third absorption component. The values obtained are presented in table 16.

TABLE 16

Number of absorbing particles in different shells

Shell	Method	Hydrogen	Helium		
		log $N_{0,2}H$	log $NH(2^1P)$	log $NH(2^3P)$	log $NH(2^1S)$
1+2	from W	15.19	14.39	14.43	13.42
	from D	15.38			
3	from W	14.76	14.31	14.25	13.79
	from D	14.98			
1+2+3	from W	15.35	14.65	14.65	13.95
	from D	15.58			

The same calculations have been made for the helium lines. The resulting values of *NH* are plotted against the upper quantum number *n* for lines of different series in figure 15. From the curves, values of *NH* for the 2^1P, 2^3P and 2^1S level can be estimated. In this case it is not possible to repeat the calculation the other way round starting from the intensity jump at the series limit nor to separate a sufficient number of lines into two components. The results are presented in table 16. The helium *NH*-values for individual shells are calculated from the *NH*-values for the total absorption and the mean ratio of equivalent widths of the first and second components for the few lines for which these are available.

6. The light variations

On the basis of the observational material presented above it is possible to discuss the light variations of P Cygni and their possible relationship to the spectral variations. Many observers have reported irregular light variations with an amplitude up to 0.2 magnitude (e.g. NIKONOV, 1936, 1937; KHARADZE *et al.*, 1952). In 1967 Magalashvili and Kharadze reported some interesting two- and three-colour observations of P Cygni. From their observations made during the period 1951–1960 they concluded that P Cygni is a W UMa system with a period of 0.500 656 days and with amplitudes of $0^m.10$ and $0^m.08$ for the primary and secondary minimum respectively (MAGALASHVILI and KHARADZE, 1967a, b).

When these results were first reported in the *Information Bulletin on Variable Stars* (No. 210) P Cygni was put on a constant observation program for 5 nights by ALEXANDER and WALLERSTEIN (1967) who reported that their observations did not reveal any variations of the brightness of P Cygni and thus did not confirm the observations made by Magalashvili and Kharadze.

It was pointed out by FERNIE (1968) that the interpretation of the half-day period in terms of binary motion is untenable because a simple calculation indicates that in this case P Cygni should have a mass of the order of 10^5 solar masses and the orbital velocity of the companion would be of the order of 10^4 km/sec. From its location in the H-R diagram and from the fact that its absolute magnitude, its colour and a half-day period would fit the observed period-luminosity-colour relationship for the β Cephei variables, Fernie suggested that P Cygni might be a β Cephei star.

It is now possible to look at the character of the light variations from a different point of view. Let us consider the conclusion of Magalashvili and Kharadze about the binary nature of P Cygni. Many decades ago the doubling of the absorption lines in the spectrum of P Cygni was considered to be evidence that this star is a binary. The two absorption components which appear at the positions of the hydrogen and helium lines are of comparable strength. This means that a companion star should not be more than one magnitude fainter than the primary star. Since the visual absolute magnitude of the system is about −8 mag, the companion also should be a very luminous star of early spectral type. One would expect that some spectral

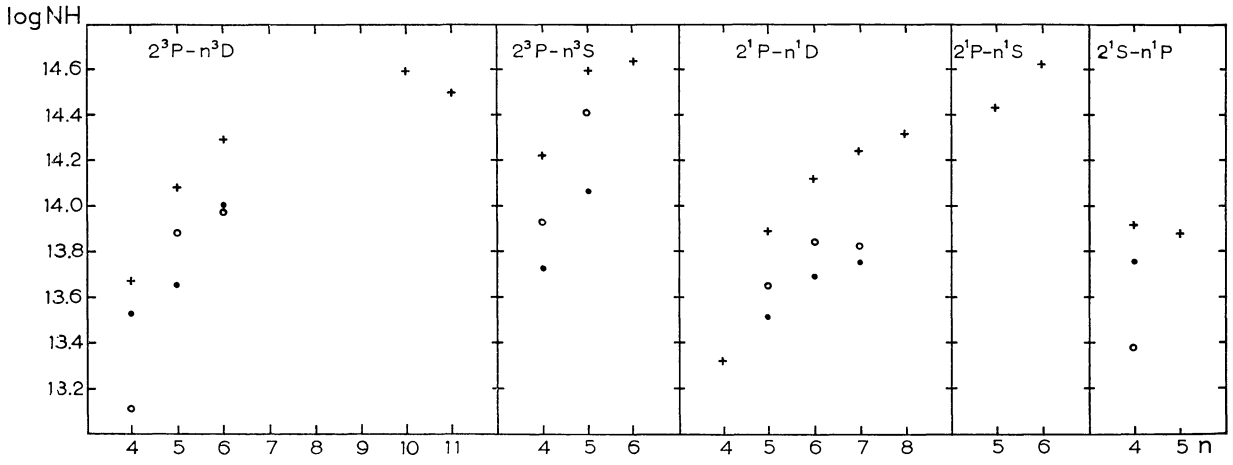

Figure 15. Log *NH* against upper quantum number *n* for some He I series. Open circles: first components; dots: second components; plus signs: unresolved first and second components.

lines other than H and He of the companion would be visible in the spectrum of P Cygni. This is not the case. Only the hydrogen and some of the helium lines are double. One might think of a late B-type companion with few strong spectral lines except those of hydrogen. But then the Si II spectrum and the line of Mg II at λ 4481 should be more prominent than the lines actually observed in the spectrum of P Cygni.

Furthermore, the mean velocity of approach, as derived from the two last absorption components of the hydrogen lines equals about −170 km/sec. If the duplicity of the lines were a proof of the binary nature of P Cygni this figure would mean either (i) that the system as a whole has a velocity of −170 km/sec with respect to the Sun, or (ii) that the W UMa binary is surrounded by a large expanding atmosphere. The first suggestion is not acceptable because it leaves unexplained the fact that all the emission lines lie at an average displacement of about −15 km/sec. Furthermore a velocity of −170 km/sec is incompatible with membership of P Cygni in the galactic cluster IC 4996. The second suggestion is difficult to maintain because the two components always fall in the same limited radial-velocity intervals between −180 and −240 km/sec and between −120 and −160 km/sec respectively, but their relative intensities change. If these were two lines from the spectra of different stars the radial velocities should pass through all values between at least −120 and −240 km/sec.

In order to find out if the intensity ratio between the second and the third absorption component or the radial velocities of these components show any correlation with the phase of the light variations given by MAGALASHVILI and KHARADZE (1967a), the phases of all the plates of this study were determined according to the period proposed by Magalashvili and Kharadze. These phases are shown in figure 16 plotted against the intensity ratio of the second and third absorption component. The intensity ratios for the Balmer lines H9, H10, H11 and H12 were used, since these lines are essentially free from blends and nearly always show the two components. The phases are shown plotted against the radial velocities of the third components of Hγ and H9 and of the second component of H9 in figure 17.

In both figures there is much scatter. In figure 16 the scatter is caused by the roughness of the visual intensity estimates that were made while measuring the spectrograms for radial velocity. In figure 17 much of the scatter is introduced by unresolved double or triple absorptions. No convincing evidence appears of a change either of the intensity ratio or of the radial velocity with a period of 0.500656 days.

The general conclusion then must be that the binary model suggested by Magalashvili and Kharadze, though very interesting from the points of view of stellar evolution and of explaining nova outbursts, is not supported by the spectroscopic information. It should be noted also that from the photometric point of view some evidence against the correctness of the conclusion of Magalashvili and Kharadze has been presented by LUUD (1969).

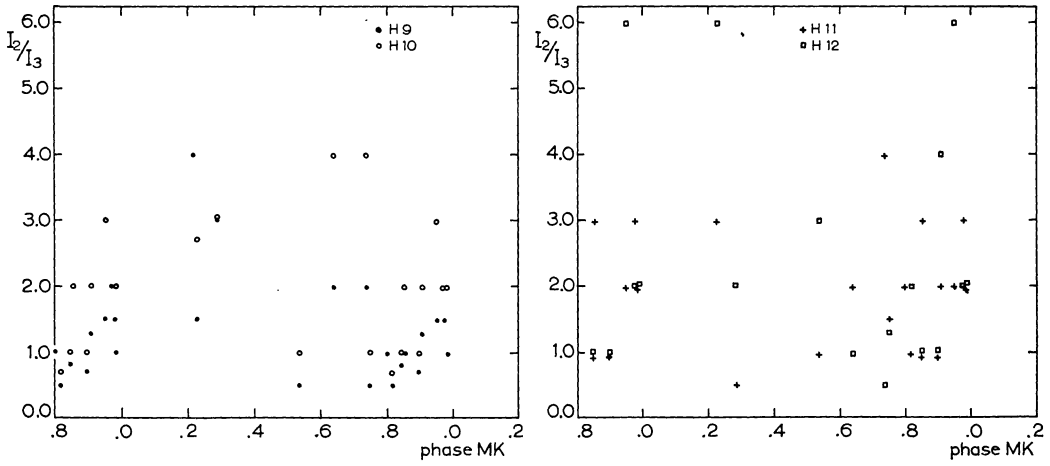

Figure 16. Intensity ratio of the second and third absorption components of some hydrogen lines against phase according to MAGALASHVILI and KHARADZE's (1967a) period.

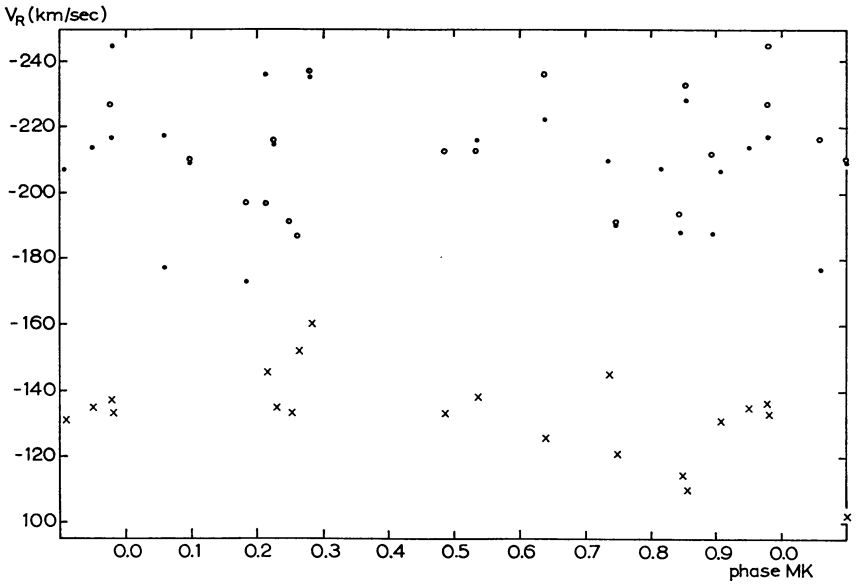

Figure 17. Radial velocity of some absorption components against phase according to MAGALASHVILI and KHARADZE's (1967a) period. Open circles: third component of Hγ; dots: third component of H9; crosses: second component of H9.

The suggestion by FERNIE (1968) that P Cygni might by a β Cephei star also is inacceptable. He calculated the visual absolute magnitude of P Cygni from his period-luminosity-colour relationship (FERNIE, 1965),

$$M_V = -5.15-3.96 \log P+6.9\,(B-V). \qquad (12)$$

His calculated visual absolute magnitude, $M_V = -7.7$ mag, is in good agreement with the observed value. If the same calculation is done with $B-V = -0.18$, the intrinsic colour of a B1Ia supergiant (JOHNSON, 1958) and with $P = 0^d.25$, which is the pulsational period of a system showing a W UMa-type light-curve with two nearly equal minima and a period of $0^d.5$, we find $M_V = -9.48$ mag. The discrepancy with Fernie's value is partly due to his using the period of $0^d.5$ of the supposed W UMa system. Furthermore Fernie must have used a value of $+0.26$ mag for the intrinsic $B-V$ colour of a B1Ia star. This is an error which can be understood by remarking that MORGAN *et al.* (1953) give -0.26 mag for the intrinsic $B-V$ colour of a B1Ia supergiant. This simple calculation shows that P Cygni does not fit Fernie's period-luminosity-colour relationship for the β Cephei stars. Also other relationships as the period-luminosity-colour and the period-luminosity relationship proposed by LEUNG (1967) do not solve this problem, so that it is concluded that the identification of P Cygni with a β Cephei star is not supported by the facts.

If P Cygni conforms to the mass-luminosity relation its visual absolute magnitude $M_V \approx -8$ mag suggests a mass of the order of 100 $M_\odot$. It has been shown by SCHWARZSCHILD and HÄRM (1959) that any star with a mass larger than 65 $M_\odot$ will be pulsational unstable with an amplitude which increases with time. This will cause the star to loose matter to interstellar space. LUUD (1967b) has suggested that this pulsational instability is the mechanism by which P Cygni looses its mass. SCHWARZSCHILD and HÄRM (1959) also computed pulsational periods for these unstable stars. They find periods ranging from $0^d.502$ for a 121 $M_\odot$ star 1.39×10^6 years after it started to burn its hydrogen fuel to $0^d.260$ for a 63 $M_\odot$ star in its initial stage. Thus the observed $0^d.25$-period may be identified with the pulsational period as a result of pulsational instability.

7. Conclusions and remarks

7.1. *Discussion*

The triple structure of the absorption lines can be explained by supposing that absorption takes place in three different shells. Of these three, the two shells closest to the star can not always be seen separately because their radial velocities differ only by a small amount; furthermore they may be close together in space. From the fact that there is a period of 114 days in the outer shell and that the average outward velocity

of the particles contributing to the third absorption component of the hydrogen lines is 210 km/sec, it is seen that in the time of one period an absorbing particle would travel about 3000 solar radii. From the relation between the visual absolute magnitude, the effective temperature and the radius, LUUD (1967b) estimated $R_* = 62\ R_\odot$ for P Cygni. Even if this value is an underestimate, matter having traveled over a distance of 3000 $R_\odot$ will have escaped from the system and will have become invisible. Therefore the shells of P Cygni are not to be compared with the shells normally seen in novae. In the case of P Cygni a shell is a much more stationary phenomenon. Nevertheless, the absorbing particles have velocities between 50 and 240 km/sec. It seems that the shells are regions in the extended atmosphere of P Cygni where the density shows a more or less permanent local maximum value. Since, however, also the equation of continuity must be fulfilled, the velocity in a dense shell must be smaller than that between the shells. This deceleration may be caused by the particles entering a shell being slowed down by frequent collisions.

The radial-velocity variations can be explained by supposing that all three shells vary with the period of 114 days. But because the amplitude of the variation reaches a high value only in the outer part of the third shell, the variation cannot be observed in lines other than the third components of the hydrogen lines. The spread of the radial-velocity measurements for the lower shells gives some idea of the amplitude of the variation at the level where the lines are formed.

We now use the derived values of $N_{0,2}H$ to draw some conclusions about the location and extent of each shell. Since the separation between the first and second shell is not well marked, only two shells are considered. From table 16 we obtain the relative $N_{0,2}H$ values for these two shells,

$$(NH)_{1,2}:(NH)_3 = 5:2. \tag{13}$$

These values for the hydrogen lines will be taken as representative for the shells as a whole since hydrogen is the most abundant element. A second relation is found in the equation of continuity

$$N_{1,2}V_{1,2}R_{1,2}^2 = N_3V_3R_3^2. \tag{14}$$

For the calculations round numbers will be used; $V_{1,2} = 120$ km/sec and $V_3 = 210$ km/sec. This gives

$$N_{1,2}R_{1,2}^2 = 1.75\ N_3R_3^2. \tag{15}$$

In order to be able to solve eqs. (13) and (15) for the relative values $N_{1,2}/N_3$, $H_{1,2}/H_3$ and $R_{1,2}/R_3$, at least one more relation is needed. It is assumed that the thickness of each shell is a function only of its distance to the centre of the star:

$$H_i \propto R_i^\beta, \tag{16}$$

where the exponent β must be chosen in such a way that the observations can be fitted into one picture. With this last assumption our set of equations reduces to

$$\left(\frac{R_3}{R_{1,2}}\right)^{\beta-2} = 0.7. \tag{17}$$

For several values of β the following values of $R_3/R_{1,2}$ are obtained:

$\beta = 0.5$, $R_3/R_{1,2} = 1.27$, $\beta = 1.25$, $R_3/R_{1,2} = 1.84$,
$\beta = 1.0$, $R_3/R_{1,2} = 1.43$, $\beta = 1.5$, $R_3/R_{1,2} = 2.57$.

In section 5.2 it was found that the relative intensity of the two components changes with a 114-day period and with opposite phases. This strongly suggests some disturbance travelling through the atmosphere with such a velocity that the distance between the two shells is covered in 57 days. Taking LUUD's (1967b) value $R_* = 62\ R_\odot$ and identifying it with the radius of the first shell (which is supposed to contribute substantially to the stellar luminosity from which the value of R_* has been derived) for $\beta = 1.5$ we find $R_3/R_{1,2} = 2.57$, which result is in agreement with the value found by STRUVE (1935) from a consideration of the dilution effects in the He I spectrum. Assembling all data, we have the following model for P Cygni:

Radius of the star $R_* \approx 50\ R_\odot$.

Radius of the first and second shell $R_{1,2} = 62\ R_\odot$.

Radius of the third shell $R_3 = 160\ R_\odot$.

Ratio of the thickness of the shells $H_3/H_{1,2} = 4.1$.

Optical thickness in Hβ of the first and second shell $(\tau_{1,2})_\beta = 18.6$; in H13: $(\tau_{1,2})_\beta = 0.20$.

Optical thickness in Hβ of the third shell $(\tau_3)_\beta = 3.72$; in H13: $(\tau_3)_\beta = 0.025$.

The last four figures were computed with the $N_{0,2}H$ values from table 16 which were determined from the Balmer jump by taking into account the finite optical

thickness of the layer. These values justify the assumption that the shells are optically thin and support the calculations made on this assumption. The fact that the outward motion of the gas is considerably in excess of the thermal Doppler motion tends to produce an optically thin situation.

With the aid of these absolute dimensions the velocity of the above-mentioned disturbance traveling through the atmosphere is about 14 km/sec. This value is remarkably close to the value of the sound velocity in a medium with $T = 20000\,^{\circ}\mathrm{K}$, $\gamma = 1.25$ and $\mu = 0.8$. It seems that sound waves traveling through the extended atmosphere play some role in the observed variation of radial velocity and of absorption line intensity. Instead of being generated by convection as in the case of solar-type stars the sound waves of P Cygni might be generated by the pulsational instability. This would nicely fit together the observed short-period light variations and the long-period radial-velocity variations.

Finally, the mass loss can be estimated from the formula

$$\mathrm{d}M = 4\pi\, R^2\, \rho(R)\, V(R)\, \mathrm{d}t. \qquad (18)$$

By virtue of the equation of continuity we can use the values of R, $\rho(R)$ and $V(R)$ for any one of the shells. Assuming that the matter in the shells is completely ionized we find from section 5.2 $\rho_{1,2} = 6\times10^{-12}\,\mathrm{g/cm^3}$ and $\mathrm{d}M = 2\times10^{-4}\ M_{\odot}$/year. This value is unexpectedly high. It agrees well with what has been found by HUTCHINGS (1969) for P Cygni and is somewhat higher than the value given by UNDERHILL (1969) for Wolf-Rayet stars. A final conclusion is that we will have to accept a rather high rate of mass loss for P Cygni and probably for the P Cygni stars in general.

7.2. *Concluding remarks*

A curve of growth analysis of the atmosphere of P Cygni has been made by LUUD (1967a, b) and by GHOBROS (1962). It seems that their work could be extended with the additional information of the present investigation. It is hoped that this new study can be undertaken as soon as the theory of line formation in an extended atmosphere like that of P Cygni is more fully understood.

If the ultimate velocity of the interstellar lines depends largely on the velocity of the stellar material sweeping away the interstellar material, it would be interesting to investigate from high-dispersion spectrograms whether the radial velocities of the circumstellar lines vary with the same period as the radial velocity of the outer shell. At the same time such a study might yield much useful information leading to a better understanding of the art of formation of circumstellar lines.

It is suspected that the spectral and light variations do not occur independently of each other. Therefore a study of the spectral variations from high-dispersion spectrograms suitably spaced in time with simultaneous multicolour photometry may reveal many more interesting facts which may contribute to a better understanding of the light and spectral variations of this peculiar star.

Acknowledgements

At the end of this investigation it is a pleasure to thank Professor Anne B. Underhill who suggested the subject to me and who by her unfaltering interest and stimulating remarks encouraged me very much. I am very much indebted to the Mount Wilson and Palomar Observatories, to the Dominion Astrophysical Observatory, to the Lick Observatory and to the Haute Provence Observatory for the loan of the many spectrograms which form the observational material underlying this study. The permission of Dr. D. Koelbloed of the Astronomical Institute of the University of Amsterdam to use their microphotometer is gratefully acknowledged. I want to thank my colleagues at the Utrecht Observatory and especially those in the Department of Stellar Spectroscopy and Photometry for the stimulating discussions they were never tired having with me. Many students have contributed to the reduction of the large amount of observational material; they did it with dedication. So did Mr. R. Staleman in drawing the figures and especially Mrs. J. Odijk-Nijenhuis who carefully typed the manuscript and the boringly long tables.

References

W. S. ADAMS, 1949, *Ap. J.* **109** 354
W. S. ADAMS and P. W. MERRILL, 1957, *Ap. J.* **125** 102
T. ALEXANDER and G. WALLERSTEIN, 1967, *Pub. Astr. Soc. Pacific* **79** 500
M. BARBIER, 1962, *Pub. Obs. Haute-Provence* **6** No. 8
D. BARBIER and D. CHALONGE, 1941, *Ann. Ap.* **4** 30
D. BARBIER, D. CHALONGE and R. CANAVAGGIA, 1947, *Ann. Ap.* **10** 195

C. S. Beals, 1930a, *Mon. Not. Roy. Astr. Soc.* **90** 202
C. S. Beals, 1930b, *Pub. Dom. Ap. Obs. Victoria* **4** 271
C. S. Beals, 1932, *Mon. Not. Roy. Astr. Soc.* **92** 677
C. S. Beals, 1934, *Pub. Dom. Ap. Obs. Victoria* **6** 125 and 144
C. S. Beals, 1935, *Mon. Not. Roy. Astr. Soc.* **95** 580
C. S. Beals, 1950, *Pub. Dom. Ap. Obs. Victoria* **9** 1
A. Belopolsky, 1899, *Ap. J.* **10** 319
K. Bockasten, 1955, *Ark. Fys.* **9** 457
K. Bockasten, 1956, *Ark. Fys.* **10** 567
A. A. Boyarchuk and I. M. Kopylov, 1958, *Soviet Astr.* **2** 752
H. E. Butler and H. Seddon, 1958, *Pub. Roy. Obs. Edinburgh* **2** 113
D. Chalonge and L. Divan, 1952, *Ann. Ap.* **15** 201
M. V. Dolidze, 1958, *Bull. Abastumanskoi Ap. Obs.* **23** 69
C. T. Elvey, 1928, *Ap. J.* **68** 416
K. B. S. Eriksson, 1957, *Ark. Fys.* **13** 303
J. D. Fernie, 1965, *Ap. J.* **142** 1072
J. D. Fernie, 1968, *Observatory* **88** 167
E. B. Frost, 1912, *Ap. J.* **35** 286
R. A. Ghobros, 1962, *Z. Ap.* **56** 113
S. Glad, 1952, *Ark. Fys.* **7** 7
S. Glad, 1956, *Ark. Fys.* **10** 291
W. M. H. Graves, E. A. Baker and R. Wilson, 1955, *Pub. Roy. Obs. Edinburgh* **1** 115
J. Grygar, 1965, *Bull. Astr. Inst. Czechoslovakia* **16** 195
G. H. Herbig, 1962, *Ap. J.* **135** 965
G. H. Herbig, 1968, *Z. Ap.* **68** 243
E. P. J. van den Heuvel, 1965, *Observatory* **85** 241
S. S. Huang and O. Struve, 1951, *Ap. J.* **121** 84
J. B. Hutchings, 1969, *Mon. Not. Roy. Astr. Soc.* (in press)
H. L. Johnson, 1958, *Lowell Obs. Bull.* **4** 37
E. K. Kharadze, 1936, *Z. Ap.* **11** 304
E. K. Kharadze, N. L. Magalashvili and T. G. Megrelishvili, 1952, *Var. Stars* **9** 150
I. D. Kupo, 1955, *Astr. Circ. S.S.S.R.* No. 163 23
H. Lamers, 1968, private communication
K. C. Leung, 1967, *Ap. J.* **150** 223
W. J. S. Lockyer, 1924, *Mon. Not. Roy. Astr. Soc.* **84** 409
L. S. Luud, 1966, *Pub. W. Struve Tartu Ap. Obs.* **35** 189
L. S. Luud, 1967a, *Soviet Astr.* **11** 211
L. S. Luud, 1967b, *Dokl. Akad. Nauk. Armenianskoi S.S.R.* **3** 379
L. S. Luud, 1969, *I.A.U. Colloquium on Non-Periodic Phenomena in Variable Stars*, Budapest 1968, in press
N. L. Magalashvili and E. K. Kharadze, 1967a, *Comm.* 27 *I.A.U., Inf. Bull. Var. Stars* No. 210
N. L. Magalashvili and E. K. Kharadze, 1967b, *Observatory* **87** 295
P. W. Merrill, 1913a, *Lick Obs. Bull.* **7** 162
P. W. Merrill, 1913b, *Lick Obs. Bull.* **8** 24
C. E. Moore, 1945, *Contr. Princeton Univ. Obs.* No. 20
C. E. Moore, 1965, *Selected Tables of Atomic Spectra*, NSRDS-NBS 3, section 1
W. W. Morgan, D. L. Harris and H. L. Johnson, 1953, *Ap. J.* **118** 92
V. B. Nikonov, 1936, *Bull. Abastumanskoi Ap. Obs.* **1** 35
V. B. Nikonov, 1937, *Bull. Abastumanskoi Ap. Obs.* **2** 23
J. D. Rosendhal, 1968, *Abstracts American Astr. Soc.*, Aug. 20–23, 1968
A. Schlüter, H. Schmidt and P. Strümpff, 1953, *Z. Ap.* **33** 194
H.Schneller, 1957, *Geschichte und Literatur des Lichtwechsels der veränderlichen Sternen* (Akademie-Verlag, Berlin)
M. Schwarzschild and R. Härm, 1959, *Ap. J.* **129** 637
O. Struve, 1935, *Ap. J.* **81** 66
A. B. Underhill, 1948, *Ap. J.* **107** 349
A. B. Underhill, 1966, *The Early Type Stars* (D. Reidel Publ. Comp., Dordrecht, Holland) p. 219 ff
A. B. Underhill, 1969, *Second Trieste Colloquium on Astrophysics: Mass Loss from Stars*, Trieste 1968, in press
A. B. Underhill and M. de Groot, 1965, *Rech. Astr. Obs. Utrecht* **17** No. 3
A. Unsöld, 1955, *Physik der Sternatmosphären* (Springer-Verlag, Berlin) 2nd ed.
R. Wilson, 1956, *Pub. Roy. Obs. Edinburgh* **2** 3
R. Wilson, 1958, *Pub. Roy. Obs. Edinburgh* **2** 61
K. O. Wright, E. K. Lee, T. V. Jacobson and J. L. Greenstein, 1964, *Pub. Dom. Ap. Obs. Victoria* **12** 173